A Mathematical Approach for Predicting Sufficient Separation Gap between Adjacent Buildings to Avoid Earthquake-Induced Pounding

Yazan Jaradat [1*], Harry Far [1], Mina Mortazavi [1]

[1] School of Civil and Environmental Engineering, Faculty of Engineering and Information Technology, University of Technology Sydney (UTS), Australia.

Abstract

Studies on earthquake-related damage underscore that buildings are vulnerable to significant harm or even collapse during moderate to strong ground motions. Of particular concern is seismic-induced pounding, observed in numerous past and recent earthquakes, often resulting from inadequate separation gaps between neighboring structures. This study conducted an experimental and numerical investigation to develop a mathematical equation to calculate a sufficient separation gap in order to avoid the collision between adjacent mid-rise steel-frame buildings during seismic excitation. In this study, the coupled configuration of 15-storey & 10-storey, 15-storey & 5-storey, and 10-storey & 5-storey steel frame structures was considered in the investigation. The investigation concluded with a large number of data outputs. The outputs were used to predict structural behavior during earthquakes. The obtained data were categorized into three main categories according to the earthquake's Peak Ground Acceleration (PGA) levels. Also, the derived equations were divided into three different equations to estimate the required seismic gap between neighboring buildings accordingly. The derived equations are distilled to empower engineers to rigorously evaluate non-irregular mid-rise steel frame buildings.

Keywords: Separation Gap; Earthquake Induced Pounding; Seismic Response; Steel Structures; Peak Ground Acceleration; Multiple Linear Regression; Finite Element Analysis.

1. Introduction

In recent times, there has been a growing interest in the issue of structural pounding between neighboring buildings during earthquakes. This concern arises due to numerous instances of building damage and collapse caused by pounding during strong earthquakes over the past two decades. One key contributing factor to this problem is the inadequate separation gap between adjacent buildings, leading to potential collisions during seismic events. This phenomenon, often referred to as "earthquake-induced structural pounding," has resulted in significant structural damage and even complete building collapses [1–3]. Furthermore, instances of local or severe damage resulting from the pounding of decks have been identified on road bridges [4–6].

The effect of structural pounding was eminent in past research works. For instance, statistical records indicated that just over 40% of the damaged or collapsed building structures during the 1985 Mexico earthquake were related to structural pounding [7]. In addition, this damage was also detected in the Loma Prieta earthquake (1989), where again remarkably 40% of the damage was due to the pounding effect [8]. Furthermore, Anagnostopoulos [9] has identified pounding damage in his work during the Northridge (1994) and Kobe (1995) quakes. Pounding criteria between adjacent building structures and resulting damage were also examined by other researchers, e.g., the Chi-Chi earthquake in 1999 [10] and the Wenchuan earthquake in 2008 [11].

Structural pounding can be classified as:

- Floor-to-floor collision [12, 13];

- Floor-to-column collision [14, 15];

- Eccentric or non-eccentric pounding [16-18];

- Pounding of heavier building with adjacent lighter building [19-21];

- Pounding between buildings in series (end building pounding) [22-24].

Earthquake-induced structural pounding takes place when the distance between structures, or structural members, cannot cover their relative dynamism and the relative lateral displacement goes beyond the separation gap [25–27]. Hence, there is a need to make calculations to ensure that there will be adequate separation gaps between adjacent buildings to avoid structural damage or collapse during earthquakes [7, 8, 28].

To mitigate the incidence of severe building damage and/or collapse brought about by earthquake-induced structural pounding, modern building codes include seismic separation requirements for adjacent structures, particularly for those places that are situated in seismically active areas. Many building rules and regulations across different countries prescribe minimum separation gaps between adjacent structures to mitigate the incidence of building collisions during earthquakes. Uniform Building Code 97 [29] introduces a method using Absolute Sums (ABS) of the maximum displacements of adjacent structures. The minimum separation distance, S, with this method is given by Equation 1:

$$S = U_a + U_b \tag{1}$$

where U_a and U_b are the maximum displacement response of buildings a and b. Considering conservative separation gap estimated by this method, Anagnostopoulos [23] suggested a method based on the Square Roots of the Sum of the Squares (SRSS) of the maximum displacements of both adjacent buildings vibrating separately (Equation 2). This equation can be found in more than one code [30, 31] and many international seismic design codes. Earlier studies have shown that this method provides conservative outcomes [32, 33]. Therefore, Jeng, et al. [32] proposed a new method on the basis of spectral difference method, known as the double difference method (DDC) or the Complete Quadratic Combination (CQC) method (Equation 3). The method is response spectrum-based and needs a correlation coefficient, ρ_{ab}, reliant on the building's period and damping ratios (Equation 4):

$$S = \sqrt{U_a{}^2 + U_b{}^2} \tag{2}$$

$$S = \sqrt{U_a^2 + U_b^2 - 2\rho_{ab}U_aU_b} \tag{3}$$

$$\rho_{ab} = \frac{8\sqrt{\xi_a\xi_b}\left(\xi_a + \xi_b\frac{T_a}{T_b}\right)\left(\frac{T_a}{T_b}\right)^{1.5}}{\left[1 - \left(\frac{T_a}{T_b}\right)^2\right]^2 + 4\xi_a\xi_b\left[1 + \left(\frac{T_a}{T_b}\right)^2\right]\left(\frac{T_a}{T_b}\right) + 4(\xi_a^2 + \xi_b^2)\left(\frac{T_a}{T_b}\right)^2} \tag{4}$$

where S is the seismic separation gap, U_a, ξ_a and T_a are the maximum displacement responses, damping ratio and natural period for building "a", and U_b, ξ_b and T_b are the maximum displacement responses, damping ratio and natural period for building "b", respectively. The DDC method has been studied by numerous researchers [33-35]. Garcia [36] studied the accuracy of the DDC method using nonlinear systems and concluded that the DDC formula provided both conservative and un-conservative results depending on adjacent building's period ratios. Hong, et al. [37] and Wang and Hong [38] enhanced the DDC technique by multiplying the coefficient based on the period ratios of the edifices. In order to accurately assess the minimum separation gap to avoid earthquake-induced pounding, Khatami, et al. [39] proposed equation to calculate the nonlinear effective period of buildings which depends significantly on the peak lateral structural response during the earthquake.

Naderpour, et al. [40] created a new method anchored on the era of adjacent buildings by altering the coefficient of correlation in the DDC method. Shrestha [41] contrasted the ABS, SRSS and DDC calculations based on the analytical required gap using linear and non-linear versions. The findings revealed that the ABS approach is conservative and overrates the gap. For the SRSS method, the outcomes were also found to be conservative when the natural periods of the adjacent structures were close to each other and not conservative when the natural periods were not similar. The DDC equation was deemed as the best method for forecasting the separation. However, only a single ground motion was applied in the research. Thus, there is a need to conduct more studies using other ground motions to validate the results. Favvata [42] examined inter-story pounding cases between an 8-storey RC frame adjacent to a 3-storey RC frame building in order to determine the minimum separation gaps for three intensity levels of seismic hazard. The required separation gap has been determined to avoid shear failure in the exterior column where the pounding is occurred. Moreover, it was established that the minimum separation distance is dependent on the level of the seismic hazard.

Barbato & Tubaldi [43] considered the DDC formula to be the most accurate, while the ABS and SRSS methods had un-conservative results. Abdel Raheem [44] in his investigation determined the distance of the gaps by utilizing three various classifications of earthquakes, to wit: low, medium, and high peak ground acceleration. The effects of the collisions were ascertained through linear elastic and non-linear contact elements among three-dimensional (3D) adjacent structures. The model showed that collision impacts can be diminished with the use of shock absorber mechanisms that address the abrupt changes during the impact. Khatami et al. [45] presented a new equation for calculating the optimal gap size to prevent structural pounding in various earthquakes. They evaluated the formula using multi-degrees of freedom models and dynamic analyses, finding it effective in determining the ideal separation distance between adjacent buildings during different seismic events.

Tena-Colunga & Sánchez-Ballinas [46] addressed Mexico City's structural pounding during the 2017 earthquake, reviewing separations in seismic codes since 1966 and reasons for enforcement gaps. A parametric study explores pounding in soft soils during 1985 and 2017 earthquakes, using equivalent frame models and evaluating well-known separation equations like ABS, SRSS, DDC, and ADC. Results suggested raising building separation distances in Mexico City's seismic code to prevent soil-related pounding, with DDC and ADC rules showing promise in aligning with dynamic simulations and being less conservative than the current absolute sum rule.

Kamal & Inel [47] investigated seismic separation gaps between adjacent low and mid-rise reinforced concrete buildings, utilizing nonlinear analysis. Models include various building heights, and nonlinear frame elements represent beam and column behaviour. 1232 analyses assess gap requirements for 56 building pairs and 11 earthquake records. The findings revealed discrepancies in code requirements for buildings with similar dynamics, and TBEC-2018 inadequacies for certain period ratios. Furthermore, two simplified approaches for gap estimation were proposed. In a related study, Kamal & Inel [48] considered soil types, showing that their new equation outperformed the Double Difference Combination (DDC) method in determining seismic gap distances across all soil types.

Other building codes appraise the height of the structure to define the sufficient separation gap between buildings. For example, the Australian code [49] recommends a minimum separation gap of 1% of the building height, h (Equation 5).

$$S = 0.01h \tag{5}$$

In their study, Jaradat et al. [50, 51] conducted experiments and numerical analyses to assess the effectiveness of the Australian standard AS1170.4-2007 in mitigating seismic pounding between steel frame structures during near-field and far-field earthquakes. Their findings revealed inaccuracies in the recommended minimum separation gap for coupled low-rise structures facing both near and far-field earthquakes. However, adequacy was observed for tall buildings, especially in far-field seismic events. Additionally, the research offers insights from results obtained through the utilisation of the ABS and SRSS methods.

The methods provided mentioned in the related literature, laws and regulations necessitate the identification of lateral displacements of the adjacent structures. The DDC method, which gives more precise findings, encompasses a correlation coefficient based on the time and damping ratios of the edifices. Supposing an engineer wants to measure the required distance using the three methods for evaluation or design, then the engineer must evaluate both edifices.

Researchers often used single-degree-of-freedom systems to simplify the issue, enabling easier structural analysis. Furthermore, existing studies were solely numerical; no experimental research was conducted. In contrast, this study broke away from the conventional approach by adopting a multiple degree of freedom (MDOF) model to represent connected structures. Through this approach, the aim was to achieve a more accurate and holistic representation of the structural behavior and response.

This study enhances existing knowledge by elucidating previous research and further streamlines engineering designs. It achieves this by establishing a clear understanding of the suitable separation gap between neighboring buildings, considering various factors like height, mass, stiffness, and structural damping. Unlike prior studies that examined one or two parameters, this research incorporates multiple building factors, employing machine learning techniques to develop a comprehensive mathematical formula.

The purpose of this study is to present a straightforward mathematical method that does not require complex analysis. Its goal is to estimate the necessary gap size to prevent earthquake-induced pounding among mid-rise steel frame buildings.

The study has employed experimental and numerical tests, utilising multi-linear regression analysis to create a predictive mathematical model for determining the necessary gap between adjacent structures to prevent earthquake-induced pounding. The investigation comprised two phases. The initial phase encompassed cross-validation between numerical and experimental data, followed by a second stage involving a parametric study. This stage examined various factors like building height, damping ratio, frequency, stiffness, mass, and earthquake inputs. Subsequent analysis, facilitated by a multiple linear regression model, was conducted once both investigation stages concluded. Figure 1 illustrates a flowchart outlining the methodology utilised in this research. This flowchart delineates the sequential steps employed to predict the regression model for ascertaining the required gap between neighboring structures, thereby averting earthquake-induced pounding.
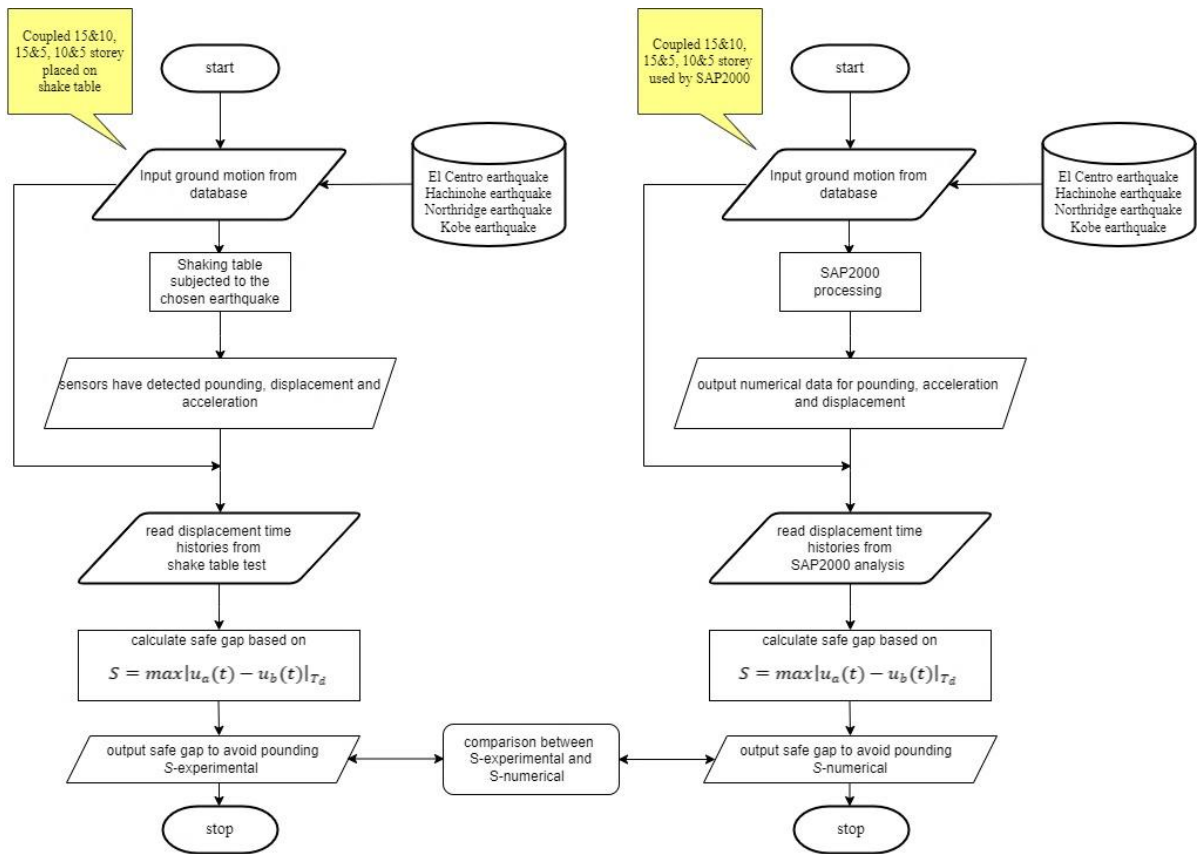
(a)
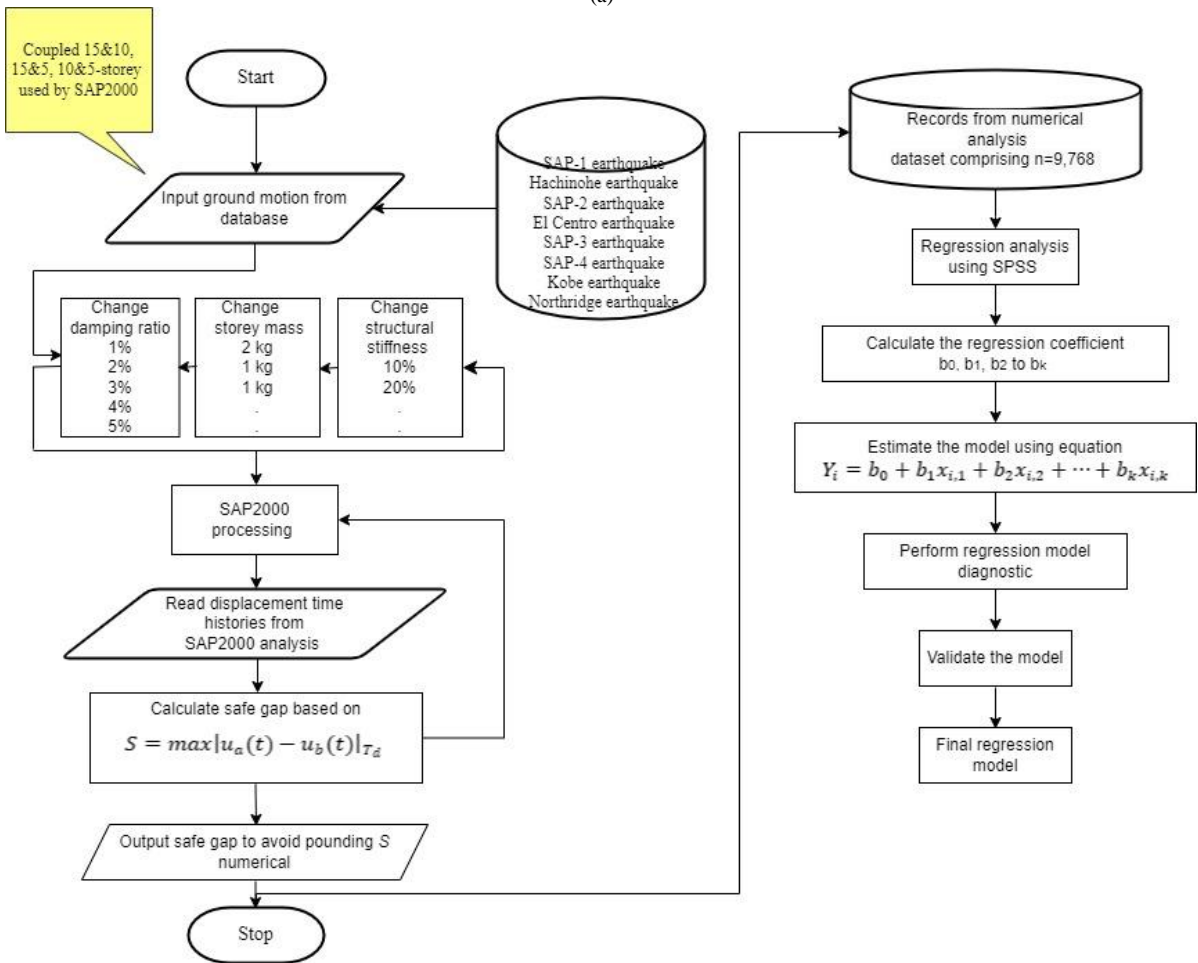
(b)

Figure 1. a) Flowchart outlining stage one methodology implementation, b) Flowchart outlining stage two methodology implementation.

2. Stage One

2.1. Tested Frames

The experiment involved 1/30 scale single-bay moment resisting steel-frame models – at 15-storey, 10-storey and 5-storey structures – on an MTS 354.20 multi-axial simulation table of size 2.2 × 2.2 m. This was done at The University of Technology, Sydney structural testing facility. The shaking table is capable of testing samples of 2 tonnes at 5 g accelerations, 1000 mm/s velocity and up to +/– 200 mm stroke. The three frame structures had individual designs done at the reduced scale in accordance to AS/NZS 3678–2011 (Structural Steel) [52]. The tested frames were designed following a similar approach as reported by Tabatabaiefar et al. [53], Tabatabaiefar & Mansoury [54]; and Tabatabaiefar [55]. The heights of the 15-storey, 10-storey and 5-storey frames were 1.5 m, 1.0 m, and 0.5 m, respectively. Columns and floors of the three models were made of rectangular flat steel sections of 40×2 mm and 400×5 mm, respectively.

2.2. Preliminary Identification Tests

The dynamic characteristics of each steel frame were identified by conducting several preliminary tests: free vibration, load-deflection, and sine sweep tests. In the free vibration test, the experiment aimed to measure the fundamental period and damping of the structures. There are different methods to measure damping. One of the methods uses the width of the peak value of the frequency response function of the structure [56]. In the load-deflection test, the experiment assessed the stiffness parameter of the frame structure [57, 58]. The sine sweep test gauged the natural frequency and modes of vibration, particularly modes 1, 2 and 3. Table 1 illustrates the characteristics of the experimental and numerical results of the 15-storey, 10-storey and 5-storey models.

Table 1. Experimental and numerical dynamic characteristics of the structural models

| Storey | Experimental | | | | | | Numerical | | | | |
| | Free Vibration | | Sine Sweep Test | | | Stiffness kN/mm | Modal Load Analysis | | | Stiffness kN/mm | Mass Kg |
	Natural Frequency Hz	Damping %	Mode 1 Hz	Mode 2 Hz	Mode 3 Hz		Mode 1 Hz	Mode 2 Hz	Mode 3 Hz		
5	6.53	0.467	7.05	21.15	36.83	0.0275	6.963	20.31	34.58	0.0276	34.85
10	3.54	0.431	3.61	11.26	18.70	0.0144	3.565	10.636	17.532	0.0149	72
15	2.27	0.503	2.31	7.11	11.76	0.0087	2.293	6.87	11.44	0.009	104

2.3. Selected Seismic Acceleration Records

Nine scaled earthquake acceleration records were used in the analyses, as depicted in Table 2. The ground motion records are grouped into three levels depending on the peak ground acceleration as, low (0.1g up to 0.3g), moderate (0.3g up to 0.6g) and high (0.6g up to 0.9g) with different dominant vibration period (T). The value of (T) can be obtained based on the calculation of Kramer [59]. In order to achieved a wide range of the period ratios (T_5/T, T_{10}/T and T_{15}/T; adjacent buildings fundamental period over the ground motion characteristic period), the earthquake acceleration records are carefully chosen. Hachinohe, El Centro, Kobe and Northridge were implemented for the shaking table tests. The four earthquakes were chosen by the International Association for Structural Control and Monitoring to benchmark seismic studies [60]. The four mentioned earthquakes were used in stage one, while more SAP earthquake records were added in stage two, and these are "SAP-1, SAP-2…. SAP-5". These SAP earthquake records were extracted from SAP2000 [61]. According to SAP2000 Time History function file, these earthquakes are real earthquakes that struck California between 1971 and 1992. The earthquake acceleration-time histories are shown in Appendix I.

Table 2. Suite of scaled earthquake ground motion records

PGA Level	PGA (g)	Earthquake	T (s)
Low	0.167	SAP-1	0.095
	0.229	Hachinohe	0.233
	0.287	SAP-2	0.182
Moderate	0.349	El Centro	0.105
	0.460	SAP-3	0.091
	0.521	SAP-4	0.063
High	0.675	Kobe	0.10
	0.849	Northridge	0.146
	0.843	SAP-5	0.125

2.4. Test Set-up

The structural models were fixed and secured on the shaking table with the configuration of 15-storey adjacent to 10-storey, 15-storey adjacent to 5-storey, and 10-storey adjacent to 5-storey. After securing the structural specimens on the shaking table, the accelerometers and laser displacement (LD) sensors were installed, as shown in Figure 2. Acceleration and displacement response data were obtained using the sensors. Moreover, an additional accelerometer was mounted on the shaking table platform to measure the applied acceleration. The acceleration time history recorded by this accelerometer was used as an input for ground motion in the numerical analyses, thereby eliminating any possible reproduction errors. The scaled earthquake acceleration records were applied to the shaking table tests. The reference frames were located outside the shaking table. Hence, the recorded displacements are the absolute displacement time history.
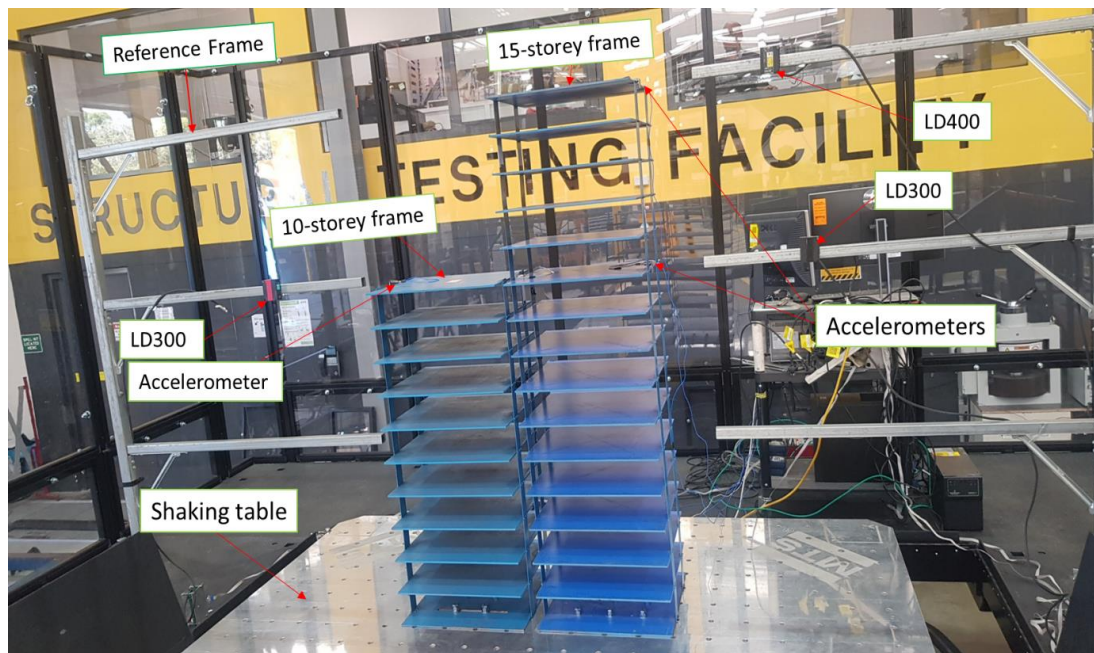

Figure 2. Test frames on shaking table

The arrangement of the sensors are as follows: for 10-storey adjacent to 5-storey steel frames, PCB 352C34 (±50 g) accelerometers were attached on the 5th and 10th floors of the 10-storey and on the 5th floor of the 5-storey frame. Laser displacement sensors were attached to the reference frames as follows: two LD300 (±150 mm) opposite to the 5th floor of both frames and an LD400 (±200 mm) opposite to 10th floor of the 10-storey frame. Similar arrangement was made for the 15-storey adjacent to 5-storey and 15-storey adjacent to 10-storey with changing the sensor location levels.

2.5. Experimental Results

The aim of this experiment is to study the safe gap between two adjacent buildings. Therefore, the impact forces due to seismic pounding have not induced and included in this experiment. The impact forces between two adjacent buildings were investigated in the authors previous article [62].

In this experiment each pair of specimens placed close to each other until pounding occurs. The pounding finally occurred when the separation distance was less than 18 mm for the 15-storey adjacent 10-storey under El Centro earthquake, less than 22mm, less than 53 mm and less than 29 mm under Hachinohe, Northridge and Kobe respectively. For the 15-storey adjacent 5-storey, the pounding occurred when the distance was less than 11 mm under El Centro earthquake, less than 13, 28 and 17 mm under Hachinohe, Northridge and Kobe earthquakes respectively. For the 10-storey adjacent -5 storey, the pounding occurred when the distance was less than 12 mm under El Centro earthquake, less than 6, 28 and 27 mm under Hachinohe, Northridge and Kobe respectively (Table 3). All the experimental program stages for pounding and no-pounding cases have been recorded and listed in Jaradat and Far [63].

3. Finite Element Modelling

3.1. Numerical Model

Three-dimensional numerical models were created in SAP2000 version 20 [61] utilising two-dimensional shell elements to model columns and floors as shown in Figure 3. Simplistic models of multi-storeyed buildings, consisting of five, ten and fifteen storey frames, are generated taking into account the material nonlinearities. The material

behaviour is considered elasto-plastic and its stress-strain relation is shown in Figure 4. The default values of the strain parameters i.e., strain at onset of strain hardening, strain at maximum stress, strain at rupture and final slope are 0.015, 0.11, 0.17 and -0.1 have been used in this study to accurately simulate the inelastic material behaviour.
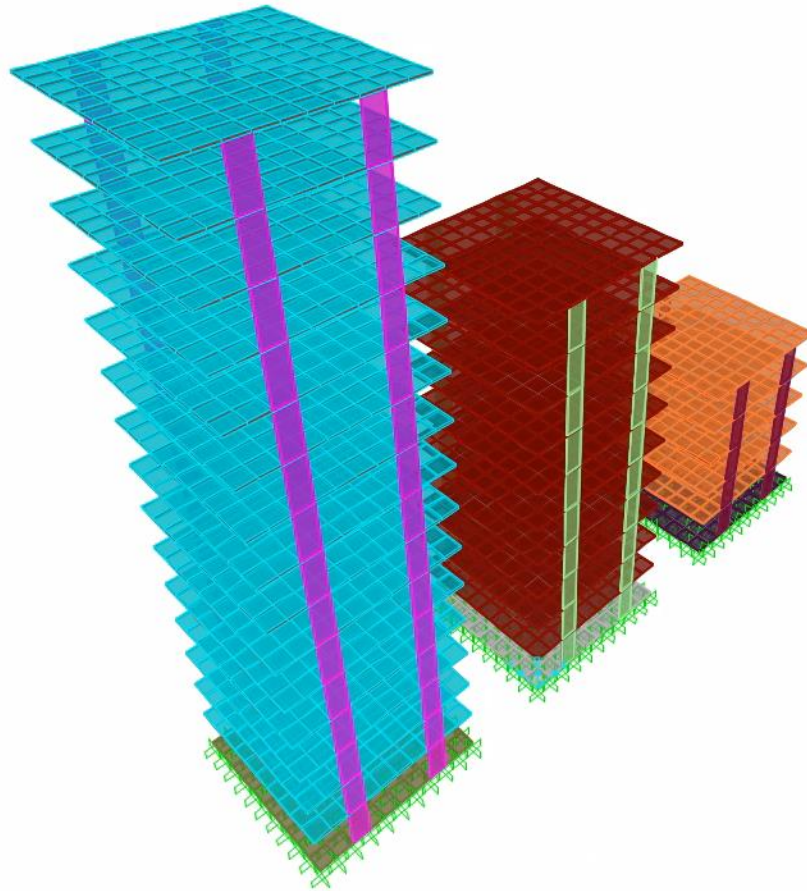

Figure 3. 3D numerical model of the structural models in SAP2000
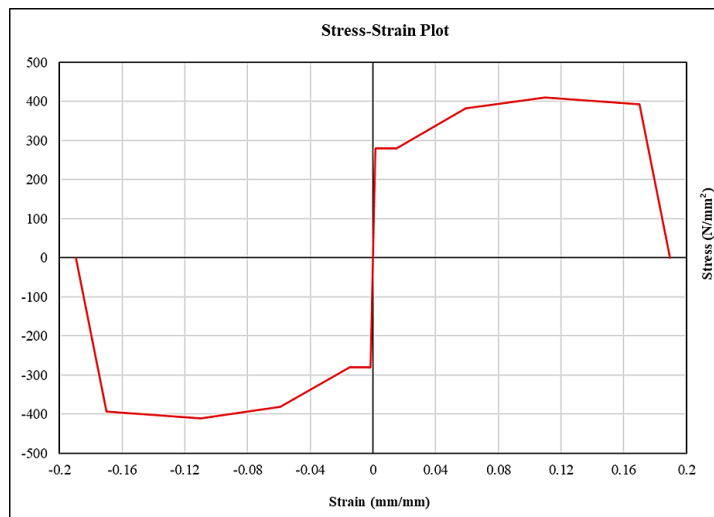
Figure 4. Stress-strain relationship for steel

The frames consist of four columns, which are modelled using vertical steel plates, with fixed boundary conditions considered at the column bases. The slabs/floors are represented using horizontal steel plates. Shell element of 2 mm and 5 mm thickness were used for the column and slap respectively.

Steel plate grade 250, according to AS/NZS 3678-2011 (Structural Steel), with a minimum yield stress of 280 MPa and a minimum tensile strength of 410 MPa, has been adopted in the design. Moreover, the Young's modulus, Poisson's ratio and mass density are taken as 200 GPa, 0.3, and 7850 kg/m^3, respectively. It is assumed that building floors are rigid in the plane level, with an even distribution of the floor mass.

The flexibility of the modelled joints can significantly impact the overall behaviour of a frame structure; thus, it is essential to correctly model the structure joints. SAP2000 offers the ability to easily fine-tune the flexibility at these joints using panel zones which are assigned to the joints themselves [64]. This includes the effects of panel zone deformation, that is, how the zone located at the intersection of a column and beam deforms. Panel zone behaviour is modelled using springs that connect the joints. In panel zone, elastic properties from column option have been used.

3.2. Numerical Analysis

Numerical analysis involving time-history used the Ritz modal loading analysis [65] to measure lateral deflection and acceleration. Ritz vectors typically capture more response when compared with the same number of Eigen vectors, Mode numbers were selected targeting dynamics check modal participating mass ratios. Nonlinear time history dynamic analyses (fast nonlinear analysis, FNA) were conducted by applying a range of 6000-11000 time steps from the subject earthquakes. FNA allows for extremely efficient and fast non-linear analysis when nonlinear behaviour is limited to predefined location. FNA is nonlinear modal time history analysis using load dependent Ritz vectors. Using Ritz vectors to perform a nonlinear time history analysis can be significantly more computationally efficient than using direct integration. However, geometric nonlinearity parameters such as P-Delta effect, have been omitted since direct integration solution was not considered.

The relative displacement of the two building structures is calculated in numerical simulations. The largest relative displacement as defined in Equation 6 is the required separation distance to avoid pounding [10].

$$S = max|u_a(t) - u_b(t)|_{T_d} \tag{6}$$

where $u_a(t)$ and $u_b(t)$ are the response time histories of adjacent buildings and T_d is the duration of vibration. *max* is the maximum value of the entire range of the relative displacement time history. The structural pounding may occur once the gap between potential pounding locations is less than *S*. In other words, pounding will occur when $u_a(t) - u_b(t) - S > 0$.

Numerical minimum separation distance to preclude pounding when 15-storey adjacent to 10-storey frames are 20, 16, 30 and 52 mm under the influence of four scaled earthquake acceleration, Hachinohe, El Centro, Kobe and Northridge, respectively. Furthermore, the minimum separation distance to avoid pounding between 15-Storey frame and 5-Storey frame are 11.5, 9, 17 and 26 mm for Hachinohe, El Centro, Kobe and Northridge, respectively. Additionally, the minimum separation distance to avoid pounding between 10-Storey frame and 5-Storey frame are 5, 10.5, 24.5 and 31 mm, under, Hachinohe, El Centro, Kobe and Northridge, respectively. These values are compared with the actual experimental results shown in Table 3.

Table 3. Experimental and numerical minimum separation distances to avoid pounding, in mm

	Hachinohe		El Centro		Kobe		Northridge	
	Experiment	Numerical	Experiment	Numerical	Experiment	Numerical	Experiment	Numerical
15S adjacent 10S	22	20	18	16	29	30	53	52
15S adjacent 5S	13	11.5	11	9	17	17	28	26
10S adjacent 5S	6	5	12	10.5	26	24.5	28	31

4. Stage Two

4.1. Selection of Structure's Parameters

In the second stage of the investigation, an intensive numerical analysis was carried out. In the previous stage, data validation was successfully completed with a negligible difference between the experimental and the numerical required separation gap. In the second stage, analyses were conducted with additional SAP earthquake records. Referring to Table 2, the earthquake records were categorised into three different levels - low, moderate and high. However, SAP-5 record was not included in the numerical analyses. It was used for validation purposes. The numerical investigation was done to determine the minimum required separation gap to prevent pounding between adjacent buildings for different parametric values, such as mass, damping ratio, natural vibration frequencies, structural stiffness and peak ground acceleration records.

When the effects of one parameter are investigated, the values of the other factors are held constant. In the analysis, the basic values of the structural models' parameters were applied as depicted in Table 1. Initially, the adjacent structures' damping ratio was gradually increased from 1% to 5%. In each level of increase, analysis was conducted to obtain the separation gap. Then, the mass was added at the centre of each floor by 2kg, 1kg, and 1kg respectively. In each level of mass increase, the analysis was done at different damping ratio. Lastly, the structure stiffness was increased by 10% and 20%. A comprehensive dataset comprising 9,768 cases was gathered to investigate separation gaps across three earthquake categories: 3,081 cases for Low PGA level, 3,081 cases for Moderate PGA level, and 3,606 cases for

High PGA level. Visual representation is provided through Tables 4 to 6, showcasing numerical separation gaps across the low, moderate, and high PGA levels. Given the substantial case count in each category, these tables focus on displaying only the initial and final records. This approach streamlines presentation while offering insight into separation gap trends across varying earthquake intensities.

Table 4. Numerical separation gap between adjacent buildings under low PGA level

Obs.	Height Tall (mm)	Height Short (mm)	PGA (g)	Frequency Tall (Hz)	Frequency Short (Hz)	Damping Tall (%)	Damping Short (%)	Stiffness Tall (kN/mm)	Stiffness Short (kN/mm)	Mass Tall (kg)	Mass Short (kg)	Numerical Min Gap (mm)
1	1500	1000	0.24	2.29	3.53	1	1	0.009	0.0149	104.2	72	14.14
2	1500	1000	0.24	2.29	3.53	1	2	0.009	0.0149	104.2	72	13.85
3	1500	1000	0.24	2.29	3.53	1	3	0.009	0.0149	104.2	72	13.62
4	1500	1000	0.24	2.29	3.53	1	4	0.009	0.0149	104.2	72	13.45
5	1500	1000	0.24	2.29	3.53	1	5	0.009	0.0149	104.2	72	13.33
6	1500	1000	0.24	2.29	3.09	1	0.431	0.009	0.0149	104.2	92	15.38
7	1500	1000	0.24	2.29	3.09	1	1	0.009	0.0149	104.2	92	15.04
8	1500	1000	0.24	2.29	3.09	1	2	0.009	0.0149	104.2	92	14.58
9	1500	1000	0.24	2.29	3.09	1	3	0.009	0.0149	104.2	92	14.25
10	1500	1000	0.24	2.29	3.09	1	4	0.009	0.0149	104.2	92	13.99
⋮						⋮						⋮
3076	1000	500	0.167	3.09	5.59	0.431	0.366	0.0149	0.0276	92	49.85	2.64
3077	1000	500	0.167	2.92	5.59	0.431	0.366	0.0149	0.0276	102	49.85	2.6
3078	1000	500	0.167	2.78	5.59	0.431	0.366	0.0149	0.0276	112	49.85	2.52
3079	1000	500	0.167	3.09	5.28	0.431	0.366	0.0149	0.0276	92	54.85	3.07
3080	1000	500	0.167	2.92	5.28	0.431	0.366	0.0149	0.0276	102	54.85	3.07
3081	1000	500	0.167	2.78	5.28	0.431	0.366	0.0149	0.0276	112	54.85	3.39

Table 5. Numerical separation gap between adjacent buildings under Moderate PGA level

Obs.	Height Tall (mm)	Height Short (mm)	PGA (g)	Frequency Tall (Hz)	Frequency Short (Hz)	Damping Tall (%)	Damping Short (%)	Stiffness Tall (kN/mm)	Stiffness Short (kN/mm)	Mass Tall (kg)	Mass Short (kg)	Numerical Min Gap (mm)
1	1500	1000	0.349	2.29	3.53	1	1	0.009	0.0149	104.24	72	14.04
2	1500	1000	0.349	2.29	3.53	1	2	0.009	0.0149	104.24	72	13.49
3	1500	1000	0.349	2.29	3.53	1	3	0.009	0.0149	104.24	72	13.06
4	1500	1000	0.349	2.29	3.53	1	4	0.009	0.0149	104.24	72	12.71
5	1500	1000	0.349	2.29	3.53	1	5	0.009	0.0149	104.24	72	12.42
6	1500	1000	0.349	2.29	3.09	1	0.431	0.009	0.0149	104.24	92	15.48
7	1500	1000	0.349	2.29	3.09	1	1	0.009	0.0149	104.24	92	15.16
8	1500	1000	0.349	2.29	3.09	1	2	0.009	0.0149	104.24	92	14.72
9	1500	1000	0.349	2.29	3.09	1	3	0.009	0.0149	104.24	92	14.35
10	1500	1000	0.349	2.29	3.09	1	4	0.009	0.0149	104.24	92	14.01
⋮						⋮						⋮
3076	1000	500	0.521	3.09	5.59	0.431	0.366	0.0149	0.0276	92	49.85	14.2
3077	1000	500	0.521	2.92	5.59	0.431	0.366	0.0149	0.0276	102	49.85	14
3078	1000	500	0.521	2.78	5.59	0.431	0.366	0.0149	0.0276	112	49.85	14
3079	1000	500	0.521	3.09	5.28	0.431	0.366	0.0149	0.0276	92	54.85	11.4
3080	1000	500	0.521	2.92	5.28	0.431	0.366	0.0149	0.0276	102	54.85	11.7
3081	1000	500	0.521	2.78	5.28	0.431	0.366	0.0149	0.0276	112	54.85	12

Table 6. Numerical separation gap between adjacent buildings under High PGA level

Obs.	Height Tall (mm)	Height Short (mm)	PGA (g)	Frequency Tall (Hz)	Frequency Short (Hz)	Damping Tall (%)	Damping Short (%)	Stiffness Tall (kN/mm)	Stiffness Short (kN/mm)	Mass Tall (kg)	Mass Short (kg)	Numerical Min Gap (mm)
1	1500	1000	0.849	2.293	3.53	1	1	0.009	0.0149	104.24	72	63.34
2	1500	1000	0.849	2.293	3.53	1	2	0.009	0.0149	104.24	72	57.4
3	1500	1000	0.849	2.293	3.53	1	3	0.009	0.0149	104.24	72	52.92
4	1500	1000	0.849	2.293	3.53	1	4	0.009	0.0149	104.24	72	49.46
5	1500	1000	0.849	2.293	3.53	1	5	0.009	0.0149	104.24	72	46.78
6	1500	1000	0.849	2.293	3.09	1	0.43	0.009	0.0149	104.24	92	46.69
7	1500	1000	0.849	2.293	3.09	1	1	0.009	0.0149	104.24	92	44.47
8	1500	1000	0.849	2.293	3.09	1	2	0.009	0.0149	104.24	92	42.22
9	1500	1000	0.849	2.293	3.09	1	3	0.009	0.0149	104.24	92	40.86
10	1500	1000	0.849	2.293	3.09	1	4	0.009	0.0149	104.24	92	39.63
⋮	⋮					⋮					⋮	
3601	1000	500	0.675	2.777	5.59	5	5	0.0149	0.0276	112	49.85	16.77
3602	1000	500	0.675	2.777	5.28	5	1	0.0149	0.0276	112	54.85	19.8
3603	1000	500	0.675	2.777	5.28	5	2	0.0149	0.0276	112	54.85	18.66
3604	1000	500	0.675	2.777	5.28	5	3	0.0149	0.0276	112	54.85	17.64
3605	1000	500	0.675	2.777	5.28	5	4	0.0149	0.0276	112	54.85	16.72
3606	1000	500	0.675	2.777	5.28	5	5	0.0149	0.0276	112	54.85	15.89

4.2. Sensitivity Analysis for Multiple Variables

To establish a multiple linear regression, it's crucial to confirm linear relationships between each independent variable and the dependent variable. This requires highlighting the significance of each variable in determining the minimum gap between structures (dependent variable). Moreover, assessing potential multicollinearity among independent variables is vital.

Multicollinearity arises from strong correlations among independent variables in regression, complicating assessment of their individual impact on the dependent variable [66, 67]. Correlations were computed via SPSS using Pearson's correlation coefficient (Pearson's r), measuring relationships between variables (-1 to +1). In this analysis, Pearson's r will be utilized alongside a two-tailed significance test.

Appendix II offers further insights into the correlation matrix. Table B.1 indicates strong correlation of mass, frequency, stiffness, and height of the short building with the minimum gap. PGA, along with tall building attributes, exhibits moderate correlation. Weak correlation is observed for damping values. This pattern is consistent across Tables B.2–B.3, confirming that short building parameters hold greater significance for the minimum gap. The analysis highlights high correlation between short building's height, frequency, stiffness, and mass. Similar correlation exists for tall building's stiffness, height, and frequency, implying multicollinearity. Despite low correlation and multicollinearity, the initial decision was to use all independent variables in a linear regression model. This enables assessing variable impact before further adjustments.

4.3. Introducing the Mathematical Models

The collected data serves to quantitatively elucidate the concept of separation gaps; a central focus detailed across Tables 4 to 6. This investigation involves a total of 12 variables, which can be categorized into one dependent variable and eleven independent variables. The independent variables, more commonly referred to as predictor variables, encompass a range of factors. Specifically, these include HT (height of the tall building in mm), HS (height of the short building in mm), E (earthquake peak ground acceleration in g), FT (frequency of the tall building in Hz), FS (frequency of the short building in Hz), DT (damping ratio of the tall building in %), DS (damping ratio of the short building in %), ST (stiffness of the tall building in kN/mm), SS (stiffness of the short building in kN/mm), MT (mass of the tall building in Kg) and MS (mass of the short building in Kg). Serving as the centrepiece, the dependent variable is symbolized as Y, embodying the minimum separation gap in millimetres. This comprehensive arrangement of variables forms the foundation upon which the intricate relationship between building characteristics and separation gaps is explored and analysed.

A Multiple Linear Regression analysis (MLR) was carried out to better understand the impact of the input variables on the output variables. MLR also known as multiple regression is a statistical technique used to explain the relationship between one dependent variable and two or more independent variables [67]. The model is estimated by least squares,

which yields parameter estimates such that the sum of squares of errors is minimized. The resulting prediction equation is shown as in Equation 7 [66]:

$$Y_i = b_0 + b_1 x_{i,1} + b_2 x_{i,2} + \cdots + b_k x_{i,k} \tag{7}$$

where, b_0 is the intercept (constant), b_1, b_2 to b_k are the regression coefficients for each explanatory (independent variable). $x_{i,k}$ are the independent (explanatory) variables. Y_i is the dependent variable or real data. The goal of using MLR in this study is to model the linear relationship between the explanatory (11 independent) variables to predict the outcome of the response (1 dependent) variable in determining the appropriate separation gap between adjacent structures to avoid earthquake induced pounding.

4.4. Estimation of Coefficients of the Model

The values of the regression coefficients of the above-mentioned model were calculated using Statistical Packages for Social Sciences (SPSS). Tables 7 to 9 display the computed regression coefficients for low, moderate, and high PGA levels. These tables also present the values of Standard Error, t-Stat, and P values. The Standard Error quantifies statistical accuracy, akin to the standard deviation of coefficient distribution or a theoretical distribution for a large population of estimates. The t-Stat is an inferential statistic, indicating if a significant difference exists between two means. The p-value (probability value), a statistical tool, gauges evidence against the null hypothesis, helping discern significant relationships or effects between variables. The null hypothesis implies no effect, while the alternative hypothesis suggests a notable effect. The regression coefficient value guides engineers and analysts in predicting one variable based on information about another. Within this study, the 11 independent variables serve as the inputs for calculating the dependent variable, which represents the suitable seismic gap between neighboring structures to prevent earthquake-induced pounding. higher regression coefficient values might indicate a significant impact from the input variables.

Table 7. SPSS regression analysis output for low PGA level

Independent Variable	Unstandardized Coefficients		t Stat	P-value
	B	Std. Error		
(Intercept)	460	25.67	17.94	1.66E-68
Height of the tall building, HT	-0.01	0.00	-10.57	1.14E-25
Height of the short building, HS	-0.28	0.02	-17.28	6.82E-64
Earthquake peak ground acceleration, E	71	1.69	42.24	1.01E-307
Frequency of the tall building, FT	-3.83	0.77	-4.97	7.12E-07
Frequency of the short building, FS	1.32	0.16	8.19	3.93E-16
Damping ratio of the tall building, DT	-0.57	0.04	-14.75	1.23E-47
Damping ratio of the short building, DS	-0.17	0.04	-4.72	2.42E-06
Stiffness of the tall building, ST	-902	127.52	-7.08	1.81E-12
Stiffness of the short building, SS	-11082	641.44	-17.28	6.64E-64
Total mass of the tall building, MT	-0.02	0.01	-1.93	0.0543
Total mass of the short building, MS	0.17	0.01	21.60	2.09E-96

Table 8. SPSS regression analysis output for moderate PGA level

Independent Variable	Unstandardized Coefficients		t Stat	P-value
	B	Std. Error		
(Intercept)	434	19.22	22.59	1.15E-104
Height of the tall building, HT	-0.004	0.00	-5.53	3.50E-08
Height of the short building, HS	-0.26	0.01	-21.37	1.49E-94
Earthquake peak ground acceleration, E	12.3	0.79	15.57	1.12E-52
Frequency of the tall building, FT	-0.85	0.58	-1.47	0.142
Frequency of the short building, FS	0.76	0.12	6.40	1.83E-10
Damping ratio of the tall building, DT	-0.64	0.03	-22.12	1.08E-100
Damping ratio of the short building, DS	-0.84	0.03	-30.59	1.25E-179
Stiffness of the tall building, ST	-578	94.98	-6.09	1.286E-09
Stiffness of the short building, SS	-10500	476.87	-22.02	6.98E-100
Total mass of the tall building, MT	0.01	0.01	1.21	0.228
Total mass of the short building, MS	0.07	0.01	11.60	1.73E-30

Table 9. SPSS regression analysis output for high PGA level

Independent Variable	Unstandardized Coefficients		t Stat	P-value
	B	Std. Error		
(Intercept)	58.8	5.96	9.88	9.61E-23
Height of the tall building, HT	-0.02	0.00	-12.38	1.61E-34
Height of the short building, HS	0.026	0.00	25.49	7E-132
Earthquake peak ground acceleration, E	48.87	0.99	49.25	0
Frequency of the tall building, FT	-0.37	1.16	-0.31	0.75
Frequency of the short building, FS	-4.39	0.26	-17.05	1.04E-62
Damping ratio of the tall building, DT	-0.995	0.06	-16.80	5.04E-61
Damping ratio of the short building, DS	-1.36	0.06	-23.73	8.6E-116
Stiffness of the tall building, ST	-1611	192.74	-8.36	9.12E-17
Stiffness of the short building, SS	0.0	0.00	65535.00	#NUM!
Total mass of the tall building, MT	0.006	0.01	0.45	#NUM!
Total mass of the short building, MS	-0.244	0.01	-18.79	3.15E-75

4.5. Testing the Significance of Regression Coefficients

In regression with multiple independent variables, the coefficient reveals how much the dependent variable is expected to increase when the independent variable increases, taking into consideration all the other independent variables remain constant. The value describes the relationship between a predictor variable and the response. To achieve this, p value is used. Based on the test, when the calculated value of (p) is less than 0.05 for the desired level of probability of (95%), the regression coefficient becomes significant. These conditions were satisfied for the development of the final mathematical model. It can be seen in Table 7 that p value of mass of the tall building, *MT,* is more than 0.05. Also, in Table 8, the p value of Frequency of the tall building, *FT,* and mass of the tall building, *MT,* are more than 0.05. Furthermore, in Table 9, the p value of Frequency of the tall building, *FT,* and Stiffness of the short building, *SS,* are more than 0.05. Therefore, the above-mentioned variables are statistically insignificant. Thus, they can be excluded from the mathematical model.

4.6. Derivation of the Mathematical Model

The statistically significant coefficients were selected from Tables 7 to 9 in order to develop the mathematical models. The mathematical model is used to predict the minimum separation gap to avoid pounding between adjacent buildings by substituting the above significant coefficient values in Equation 7. Based on the results of the regression analysis, the following linear equations are developed and proposed:

For low PGA level:

$$\hat{Y}_1 = 460 - 0.01 \times HT - 0.28 \times HS + 71 \times E - 3.83 \times FT + 1.32 \times FS - 0.57 \times DT - 0.17 \times DS - 902 \times ST - 11082 \times SS + 0.17 \times MS \tag{8}$$

For moderate PGA level:

$$\hat{Y}_1 = 434 - 0.004 \times HT - 0.26 \times HS + 12.3 \times E + 0.76 \times FS - 0.64 \times DT - 0.84 \times DS - 578 \times ST - 10500 \times SS + 0.07 \times MS \tag{9}$$

For high PGA level:

$$\hat{Y}_1 = 58.8 - 0.02 \times HT + 0.026 \times HS + 48.87 \times E - 4.39 \times FS - 0.99 \times DT - 1.36 \times DS - 1611 \times ST + 0.006 \times MT - 0.244 \times MS \tag{10}$$

where $\hat{Y}_1$ is the predicted data (the predicted minimum separation gap using Equations 8 to 10.

There are 11 independent variables, for which frequency, mass, and stiffness depends on each other. These parameters were obtained individually using the experimental model. The MLR analysis was done by excluding in certain cases, the frequency and keeping mass and stiffness, excluding stiffness and keeping frequency and mass, or excluding mass and keeping frequency and stiffness. These steps were carried out in order to minimise the mathematical model variables and to increase its accuracy. Sections 4.3 and 4.4 have been repeated for excluding stiffness and mass then frequency and stiffness. Tables 10 and 11 illustrate the regression coefficients for low PGA level, excluding

stiffness and mass, and frequency and stiffness. Tables 12 and 13 illustrate the regression coefficients for moderate PGA level, excluding stiffness and mass, and frequency and stiffness. Tables 14 and 15 illustrate the regression coefficients for high PGA level, excluding stiffness and mass, and frequency and stiffness.

Table 10. SPSS regression analysis output for low PGA level, excluding stiffness & mass

Independent Variable	Unstandardized Coefficients		t Stat	P-value
	B	Std. Error		
(Intercept)	23	1.668	13.823	3.3E-42
Height of the tall building, HT	-0.005	0.001	-8.796	2.3E-18
Height of the short building, HS	-0.001	0.001	-1.129	0.26
Earthquake peak ground acceleration, E	57.8	1.650	35.018	2.3E-226
Frequency of the tall building, FT	-4.08	0.237	-17.209	1.96E-63
Frequency of the short building, FS	-1.7	0.113	-15.306	5.0E-51
Damping ratio of the tall building, DT	-0.57	0.044	-13.160	1.6E-38
Damping ratio of the short building, DS	-0.14	0.039	-3.522	0.00043

Table 11. SPSS regression analysis output for low PGA level, excluding frequency & stiffness

Independent Variable	Unstandardized Coefficients		t Stat	P-value
	B	Std. Error		
(Intercept)	-14	0.59	-23.86	1.3E-115
Height of the tall building, HT	-0.0001	0.00	-0.38	0.7
Height of the short building, HS	-0.0023	0.00	-4.18	2.9E-05
Earthquake peak ground acceleration, E	57	1.58	35.94	1.7E-236
Damping ratio of the tall building, DT	-0.59	0.04	-14.22	1.6E-44
Damping ratio of the short building, DS	-0.06	0.04	-1.71	0.087
Total mass of the tall building, MT	0.04	0.00	15.52	2.4E-52
Total mass of the short building, MS	0.13	0.01	24.77	1.0E-123

Table 12. SPSS regression analysis output for moderate PGA level, excluding stiffness & mass

Independent Variable	Unstandardized Coefficients		t Stat	P-value
	B	Std. Error		
(Intercept)	16	1.16	14.06	1.5E-43
Height of the tall building, HT	-0.002	0.00	-3.82	0.00014
Height of the short building, HS	0.008	0.00	13.74	9.3E-42
Earthquake peak ground acceleration, E	3	0.73	4.16	3.3E-05
Frequency of the tall building, FT	-2.2	0.17	-12.80	1.4E-36
Frequency of the short building, FS	-0.24	0.09	-2.74	0.006
Damping ratio of the tall building, DT	-0.65	0.03	-20.84	2.3E-90
Damping ratio of the short building, DS	-0.91	0.03	-30.54	3.6E-179

Table 13. SPSS regression analysis output for moderate PGA level, excluding frequency & stiffness

Independent Variable	Unstandardized Coefficients		t Stat	P-value
	B	Std. Error		
(Intercept)	2	0	5	6.0E-06
Height of the tall building, HT	0.001	0.00	3.04	0.0024
Height of the short building, HS	0.007	0.00	14.64	5.9E-47
Earthquake peak ground acceleration, E	4	0.73	5.61	2.2E-08
Damping ratio of the tall building, DT	-0.66	0.03	-21.21	2.5E-93
Damping ratio of the short building, DS	-0.87	0.03	-29.12	7.4E-165
Total mass of the tall building, MT	0.02	0.00	12.19	2.0E-33
Total mass of the short building, MS	0.03	0.00	7.01	2.8E-12

Table 14. SPSS regression analysis output for high PGA level, excluding stiffness & mass

Independent Variable	Unstandardized Coefficients		t Stat	P-value
	B	Std. Error		
(Intercept)	-0.83	2.46	-0.3	0.74
Height of the tall building, HT	-0.009	0.001	-11	4.7E-28
Height of the short building, HS	0.024	0.001	22	1.5E-102
Earthquake peak ground acceleration, E	49	1	47	0
Frequency of the tall building, FT	-3.4	0.3	-10.1	1.3E-23
Frequency of the short building, FS	-0.6	0.2	-3.5	0.0004
Damping ratio of the tall building, DT	-1.0	0.1	-15.7	1.6E-53
Damping ratio of the short building, DS	-1.2	0.1	-20.6	2.5E-89

Table 15. SPSS regression analysis output for high PGA level, excluding frequency & stiffness

Independent Variable	Unstandardized Coefficients		t Stat	P-value
	B	Std. Error		
(Intercept)	-24	1	-24	4.3E-119
Height of the tall building, HT	-0.005	0.00	-8.71	4.6E-18
Height of the short building, HS	0.03	0.00	36.33	1.8E-246
Earthquake peak ground acceleration, E	49	1	47	0
Damping ratio of the tall building, DT	-1.0	0.06	-15.87	6.6E-55
Damping ratio of the short building, DS	-1.2	0.06	-20.47	3.2E-88
Total mass of the tall building, MT	0.04	0.00	8.82	1.7E-18
Total mass of the short building, MS	-0.07	0.01	-8.31	1.3E-16

The new mathematical equations for low PGA level are:

$$\hat{Y}_2 = 23 - 0.005 \times HT + 57.77 \times E - 4.08 \times FT - 1.7 \times FS - 0.57 \times DT - 0.138 \times DS \tag{11}$$

$$\hat{Y}_3 = -14 - 0.0023 \times HS + 57 \times E - 0.59 \times DT + 0.04 \times MT + 0.13 \times MS \tag{12}$$

The new mathematical equations for moderate PGA level are:

$$\hat{Y}_2 = 16 - 0.002 \times HT + 0.008 \times HS + 3 \times E - 2.2 \times FT - 0.24 \times FS - 0.65 \times DT - 0.91 \times DS \tag{13}$$

$$\hat{Y}_3 = 2 + 0.001 \times HT + 0.007 \times HS + 4 \times E - 0.66 \times DT - 0.87 \times DS + 0.02 \times MT + 0.03 \times MS \tag{14}$$

The new mathematical equations for high PGA level are

$$\hat{Y}_2 = -0.83 - 0.009 \times HT + 0.024 \times HS + 49 \times E - 3.4 \times FT - 0.6 \times FS - DT - 1.2 \times DS \tag{15}$$

$$\hat{Y}_3 = -24 - 0.005 \times HT + 0.03 \times HS + 49 \times E - DT - 1.2 \times DS + 0.04 \times MT - 0.07 \times MS \tag{16}$$

where $\hat{Y}_2$ is the predicted data (the predicted minimum separation gap using Equations 11 or 13 or 15) and $\hat{Y}_3$ is the predicted data (the predicted minimum separation gap using Equations 12 or 14 or 16.

4.7. Cross Validation Technique

Cross validation is a statistical method of evaluating how the results of a projected model will validate the real data set. The technique is used when one intends to evaluate and compare how precise a predictive model is when applied into real data [68]. In this study, two methods of cross validation were used in Equations 17 and 18. The Mean Square Error (MSE), represents how close a regression line is to a set of points (the distances are the "errors"). MSE provides the average of the square of the difference between actual and estimated values. The other one is the Mean Absolute Error (MAE) gives the mean of absolute difference between model prediction and target value. MAE is the magnitude of difference between the prediction of an observation and actual data or true value of that observation. Lower values mean stronger attainment of the mathematical model (zero means no error). MSE is expressed in Equation 17, while MAE is shown in Equation 18:

$$MSE = \sum(Y_i - \hat{Y}_i)^2 / N \tag{17}$$

$$MAE = \sum|Y_i - \hat{Y}_i| / N \tag{18}$$

where Y_i is the actual data, $\hat{Y}_i$ is the predicted data (the predicted minimum separation gap using the mathematical model), N is the number of observations. Table 16 shows MSE and MAE for the above developed mathematical models under different PGA intensity.

Table 16. MSE and MAE comparison of the developed mathematical models

	Low PGA Level		Moderate PGA Level		High PGA Level	
	MSE	**MAE**	**MSE**	**MAE**	**MSE**	**MAE**
$\hat{Y}_1$	31.11	4.97	11.71	2.93	30.42	4.67
$\hat{Y}_2$	13.3	2.67	7.09	1.84	30.28	4.39
$\hat{Y}_3$	12.02	2.47	6.59	1.82	38.85	4.59

Based on the values of MSE and MAE in Table 16, the mathematical model revealed that the lowest value for MSE and MAE is the best fit model. Therefore, for low, moderate, and high PGA levels, the best-chosen models are indicated as in Equations 12 to 15, respectively. In the succeeding sections, the different developed models will be validated for the structural parameters.

5. Validation Processes and Results

To validate the method for other structural factors, the study was expanded to buildings with various heights, masses, and stiffness of each level for both structures. This section describes an illustrative example of the validation analysis carried out for 12-storey building adjacent to 8-storey building and 10-storey building adjacent to 8-storey building. The adjacent buildings are exposed to the SAP-2 earthquake record (PGA = 0.287 g), the SAP-3 earthquake record (PGA = 0.46 g) and the SAP-5 earthquake record (PGA = 0.843 g) for low, moderate and high PGA levels, respectively. The 12-storey and 8-storey buildings were designed in similar steps as in the previous models. In the analysis, the following basic values of the structural model's parameters have been applied. For 12-storey building (height = 1200 mm, natural frequency = 2.984 Hz, stiffness = 0.0125 kN/mm and mass = 84.5 kg) and for 8-storey building (height = 800 mm, natural frequency = 4.317 Hz, stiffness = 0.0185 kN/mm and mass = 58 kg). Then, similar steps were applied as section 4.1 to obtain numerical minimum separation gap.

Figure 5 compares separation gaps between 12-story adjacent to 8-story and 10-story adjacent to 8-story buildings during the SAP-2 earthquake. Equation 8 predictions significantly deviate from actual data, while Equations 11 and 12 closely match observed values. In the 12-story adjacent to 8-story case, Equations 11 and 12 yield MSE and MAE values of (30, 6.03) and (24.3, 4.5), respectively. For 10-story adjacent to 8-story buildings, they yield (16.8, 4.3) and (16.4, 3.6). Remarkably, Equations 11 and 12 exhibit similar MSE and MAE values. Thus, due to its simplicity and accuracy, Equation 11 is recommended as the best-fit mathematical model for predicting minimum separation gaps in low PGA areas.
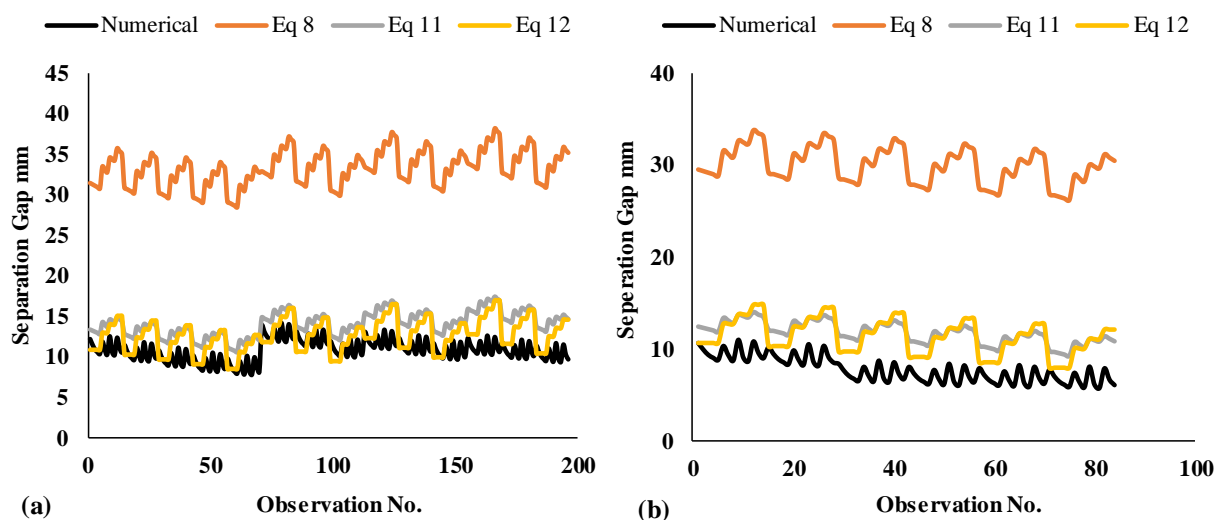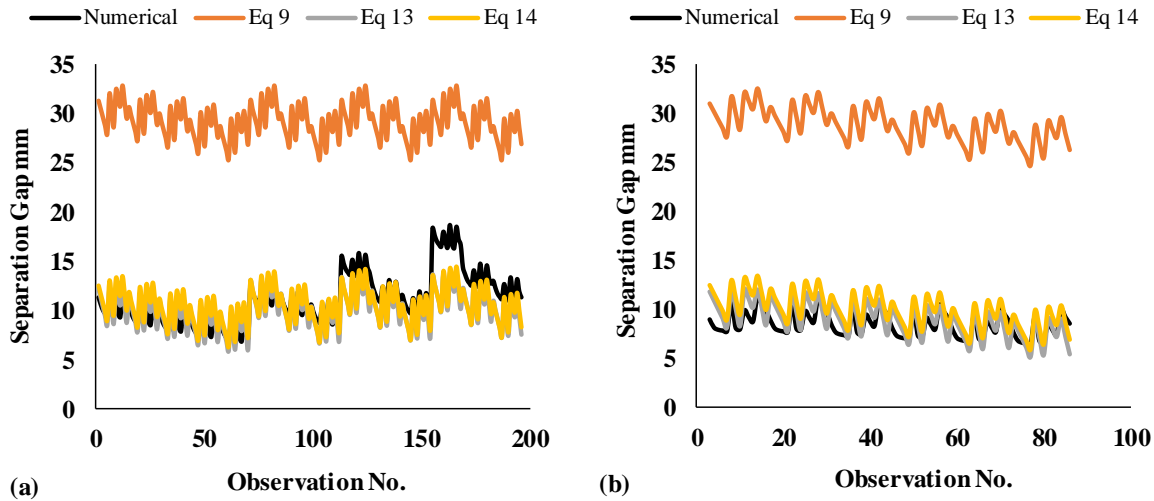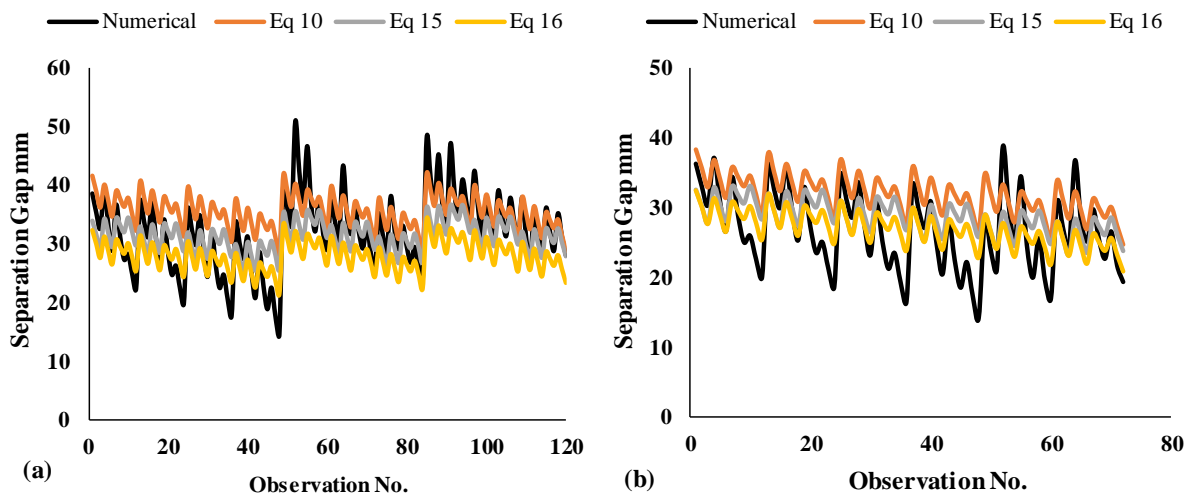

Figure 5. Example of the results of the validation analysis for low PGA level under SAP-2 earthquake record; a) 12-storey adjacent 8-storey, b) 10-storey adjacent 8-storey

Building on these observation, Figure 6 illustrates the separation gaps during the SAP-3 earthquake, considering 12-story adjacent to 8-story and 10-story adjacent to 8-story buildings. Notably, Equation 9 predictions significantly deviate from actual data, whereas Equations 13 and 14 closely approximate observed values. In the context of 12-story adjacent to 8-story buildings, Equations 13 and 14 yield MSE and MAE values of (0.83, 1.53) and (1.94, 1.57), respectively. For 10-story adjacent to 8-story structures, they result in (1.87, 1.13) and (3.63, 1.66) for MSE and MAE, respectively. Remarkably, Equation 13 displays the lowest MSE and MAE. Consequently, Equation 13 stands as the best-fitting mathematical model for predicting minimum separation gaps in areas characterized by moderate PGA levels.

Figure 6. Example of the results of the validation analysis for moderate PGA level under SAP-3 earthquake record; a) 12-storey adjacent 8-storey, b) 10-storey adjacent 8-storey

Expanding the analysis in Figure 7, which presents the separation gaps observed during the SAP-5 earthquake for 12-story adjacent to 8-story and 10-story adjacent to 8-story buildings. Evidently, Equations 10, 15, and 16 provide accurate predictions for the separation gap. For 12-story adjacent to 8-story structures, the MSE and MAE values for Equations 10, 15, and 16 are (33.57, 4.6), (24.83, 3.96), and (37.55, 5.25), respectively. In the case of 10-story adjacent to 8-story buildings, they result in (42.04, 3.49), (28.5, 5.73), and (18.05, 6.72) for MSE and MAE, respectively. Notably, Equation 10 yields the lowest MSE and MAE values, establishing it as the best-fit mathematical model for predicting minimum separation gaps in areas characterised by high PGA levels.

Figure 7. Example of the results of the validation analysis for high PGA level under SAP-5 earthquake record; a) 12-storey adjacent 8-storey, b) 10-storey adjacent 8-storey

6. Regression Model Improvements

The Regression Model can be enhanced in many instances by increasing or reducing factors and interactions in the analysis selection [69]. In order to enhance the accuracy and improve the prediction of the developed mathematical

models, a series of methods were carried out till a better fit model was developed. Reviewing the previous section indicates that the mathematical model for low and high PGA levels can be enhanced to improve their accuracy. Whereas, the mathematical model output for the moderate PGA level was accurate since the MAE and MSE were very low. Hence, there is no need for any improvements to be done.

6.1. Low PGA Level

From the above analysis, the selected mathematical model for low PGA level is expressed in Equation 11. The researchers introduced a new variable to be used in the regression analysis: squared value of the earthquake peak ground acceleration, E^2 this variable was used after conducting many trials. The new regression coefficients are illustrated in Table 17. The enhanced mathematical model is expressed in Equation 19. The values of MSE and MAE for the equation were reduced from 13.3 to 9.67 and from 2.67 to 2.14, respectively.

Table 17. SPSS regression analysis output of the enhanced mathematical model for low PGA level

Independent Variable	Unstandardized Coefficients		t Stat	P-value
	B	Std. Error		
(Intercept)	-50.7	2.76	-18.37	1.3E-71
Height of the tall building, HT	-0.0028	0.00	-5.45	5.3E-08
Height of the short building, HS	0.0066	0.00	9.59	1.8E-21
Earthquake peak ground acceleration, E	600	17.35	34.64	3.2E-222
Frequency of the tall building, FT	-3.59	0.21	-17.40	9.6E-65
Frequency of the short building, FS	-0.46	0.11	-4.36	1.3E-05
Damping ratio of the tall building, DT	-0.64	0.04	-16.93	1.5E-61
Damping ratio of the short building, DS	-0.5	0.04	-13.94	7.4E-43
Squared earthquake peak ground acceleration, E^2	-1210	38.53	-31.41	4.3E-188

$$\hat{Y}_i = -50.7 - 0.0028 \times HT + 0.0066 \times HS + 600 \times E - 3.59 \times FT - 0.46 \times FS - 0.64 \times DT - 0.5 \times DS - 1210 \times E^2 \tag{19}$$

To validate the new enhanced model, section 5 will be repeated for low PGA level exposed to the SAP-2 earthquake record. It can be seen in Figure 8 that the predicted separation gap using Equation 19 is closer to the actual numerical data compared to the prediction by Equation 11. The calculated MSE and MAE for Equation 19 in 12-storey adjacent to 8-storey buildings are (2.65, 1.2). While the MSE and MAE for Equation 19 in 10-storey adjacent to 8-storey buildings are (1.22, 0.96). These very low values of error indicate that the enhanced model performs well and its accuracy has improved.
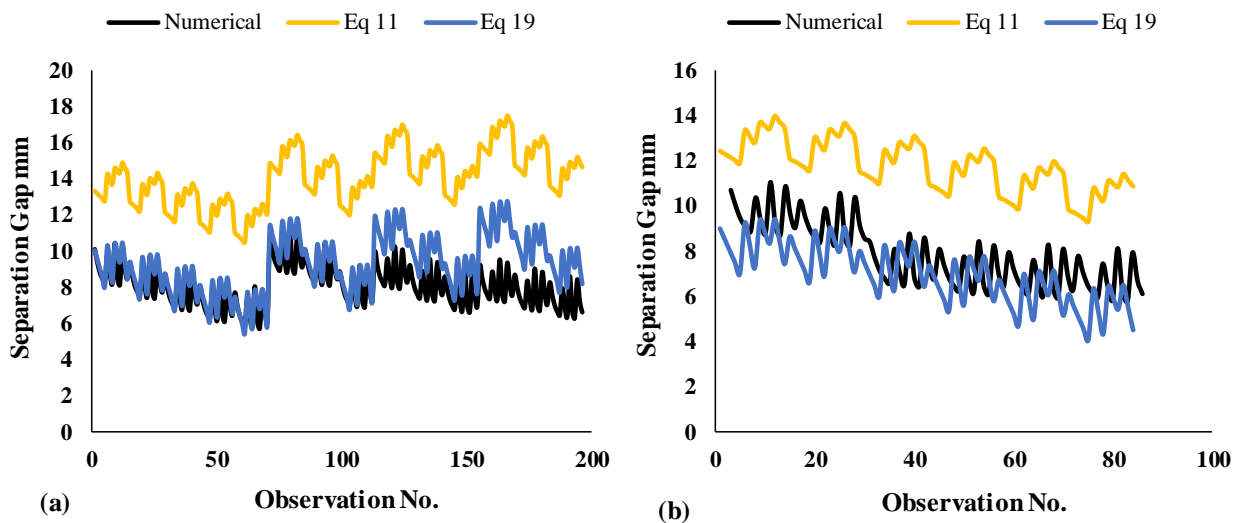

Figure 8. Validation analysis for low PGA level for the enhanced model under SAP-2 earthquake record; a) 12-storey adjacent 8-storey, b) 10-storey adjacent 8-storey

6.2. High PGA Level

From the above analysis, the selected mathematical model for high PGA level is reflected in Equation (15). Polynomial regression is special case of multiple linear regression which approximates the relationship between the independent and dependent variables depicted as an nth degree polynomial [70]. Referring to equation 15, the dependent variable output, $\hat{Y}_2$, was used as an independent variable in this polynomial equation as shown in Figure 9. Therefore, the enhanced mathematical model is expressed in Equation 20. The values of MSE and MAE for the equation has dropped from 30.28 to 15.74 and from 4.39 to 3.05, respectively.

$$\hat{Y}_i = 0.054 \times \hat{Y}_2{}^2 - 1.64 \times \hat{Y}_2 + 29.06 \tag{20}$$
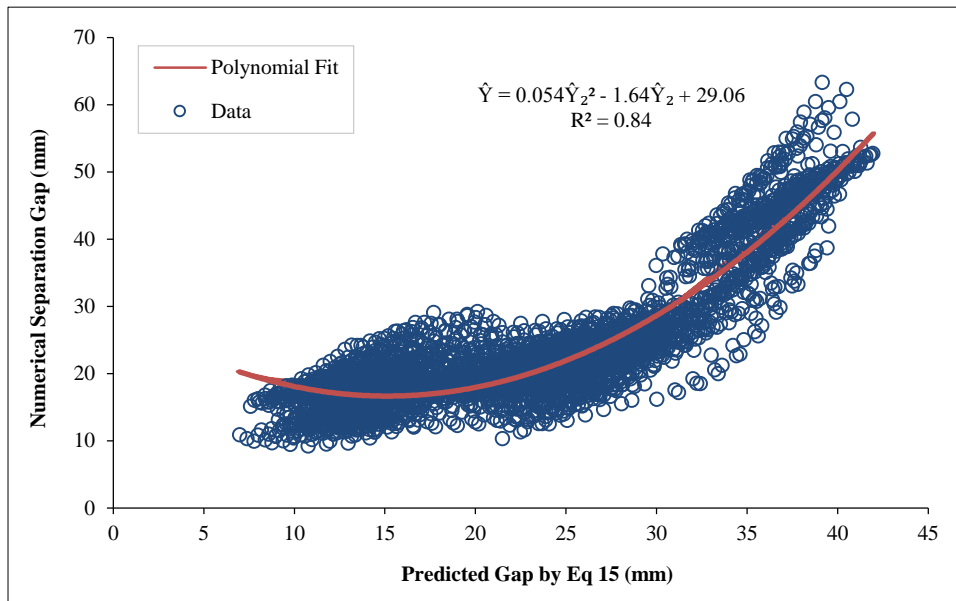
Figure 9. Scatter chart between numerical gap and predicted gap using Equation (15)

To validate the new enhanced model, the procedure defined in section 5 will be repeated for high PGA level exposed to the SAP-5 earthquake record. It can be seen in Figure 10 that the predicted separation gap using Equation 20 is closer to the actual numerical data compared to the prediction by Equation 15. The calculated MSE and MAE for Equation 20 in 12-storey adjacent to 8-storey buildings are 19.36 and 3.59. While the MSE and MAE for Equation (20) in 10-storey adjacent to 8-storey buildings are 24.11 and 3.19. The very low values of error indicated that the new enhanced model performs better and the accuracy has progressed.
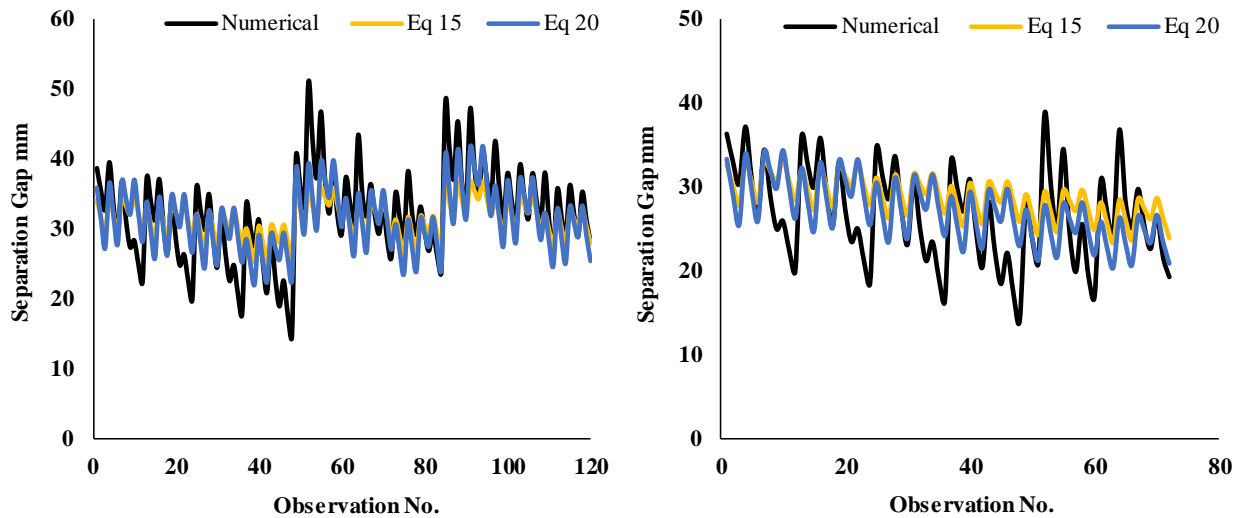

Figure 10. Validation analysis for high PGA level for the enhanced model under SAP-5 earthquake record; a) 12-storey adjacent 8-storey, b) 10-storey adjacent 8-storey

7. Comparative Assessment of Newly Developed Mathematical Models

To assess the efficacy of the newly formulated mathematical models—referred to as Equation 19, Equation 13, and Equation 20—for varying levels of PGA (low, moderate, and high), a comparative analysis will be conducted. The outcomes generated by these specified equations will be compared against the results derived from the ABS and SRSS techniques. The comparative evaluation will be visualised through Figures 11 to 13, illustrating a contrast between the outcomes of the developed mathematical equations and those produced by the ABS and SRSS methods. This comparison pertains to the computation of the minimum separation gap required to prevent earthquake-induced pounding between a 12-story and an 8-story building situated adjacently. The depicted figures reveal a notable similarity between the outcomes produced by the suggested mathematical equations and the SRSS method, in contrast to the results yielded by the ABS approach. These observations align with the conclusions drawn by Jeng, et al. [71], Kasai, et al. [72], Lopez-Garcia & Soong [34] and Jaradat, et al. [50].
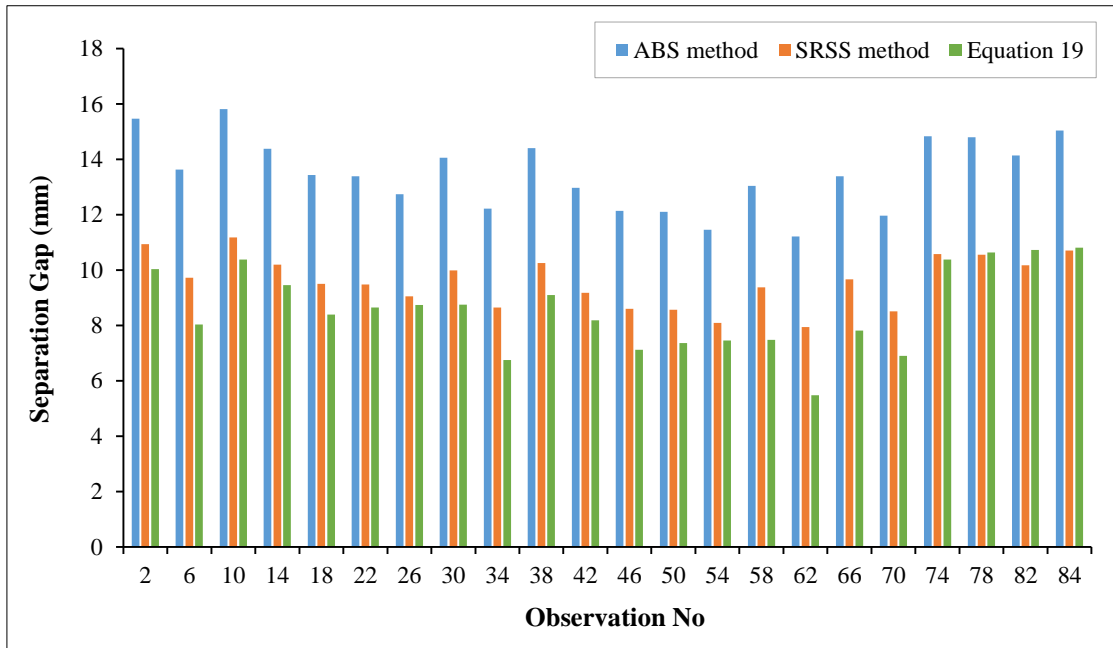
Figure 11. Minimum separation gap calculated by different methods between 12-storey adjacent 8-storey subjected to SAP-2 earthquake record, for low PGA level
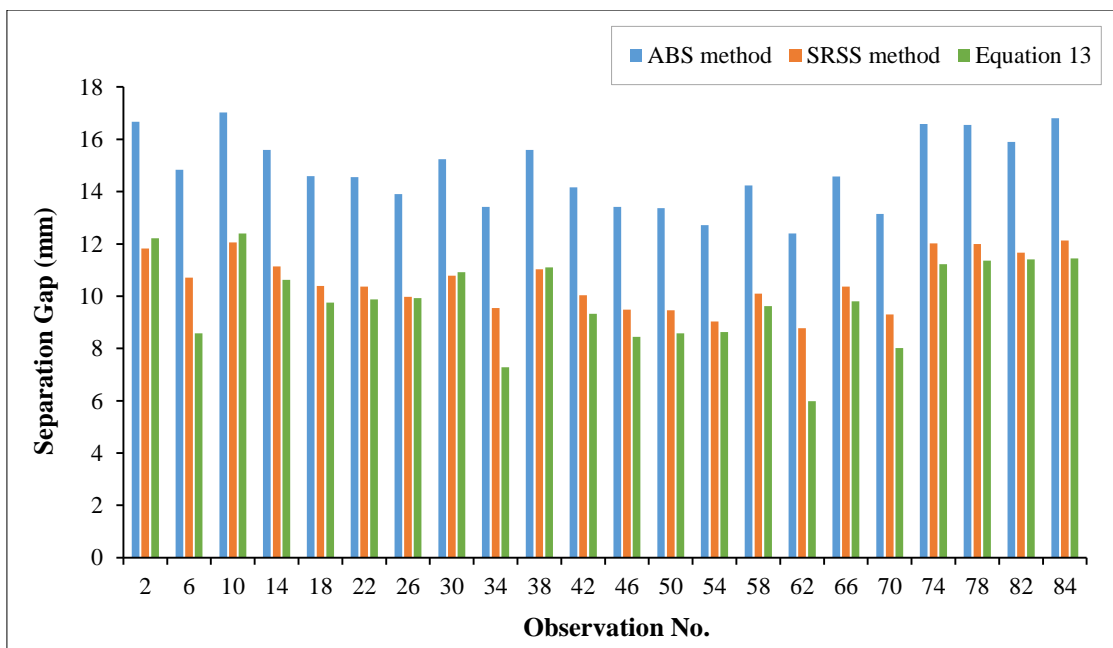

Figure 12. Minimum separation gap calculated by different methods between 12-storey adjacent 8-storey subjected to SAP-3 earthquake record, for moderate PGA level
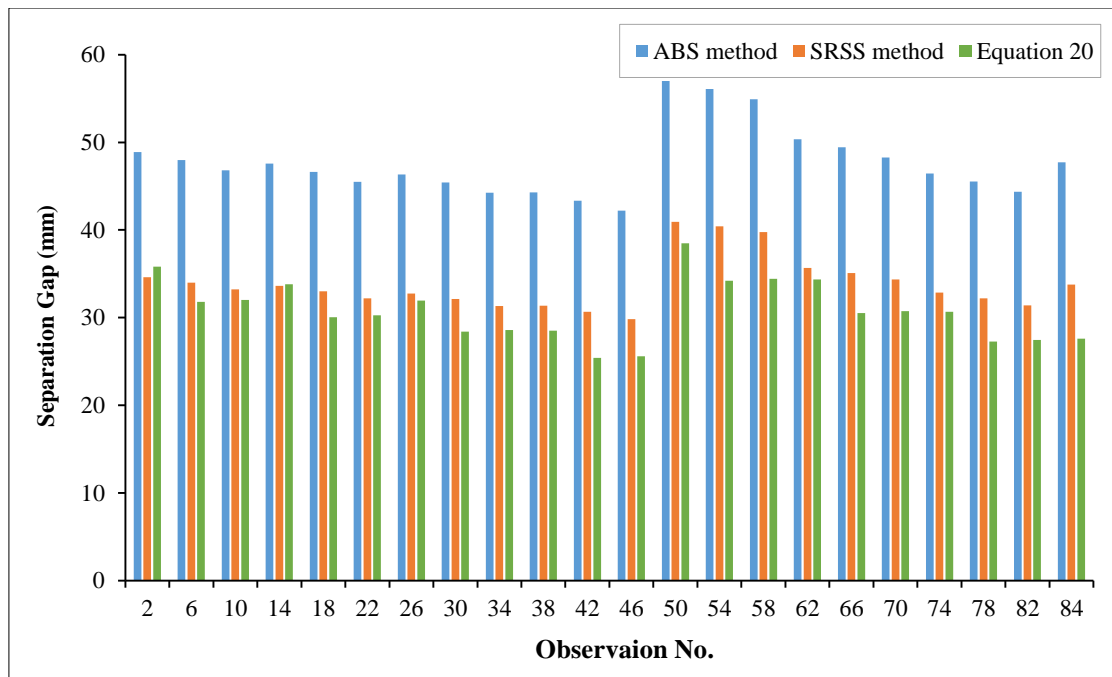
Figure 13. Minimum separation gap calculated by different methods between 12-storey adjacent 8-storey subjected to SAP-5 earthquake record, for high PGA level

8. Simplified Procedure for Practical Application

8.1. General

Many research works have been conducted to mitigate the incidence of pounding hazards during earthquakes. One of the objectives is to develop processes for assessing sufficient separation distance between structures to prevent contact during seismic excitations [33]. The minimum separation gap is clearly defined in most recent seismic-resistant design codes, such as UBC 1997, Euro-Code 2005, IBC 2009 and AS1170.4. The aim for this provision is to improve the seismic performance of current edifices with insufficient in-between space and to establish adequate techniques to lessen the pounding effects on structural members.

Earthquake induced structural pounding between adjacent edifices is a complicated phenomenon involving plastic deformations at contact points, local cracking or crushing, fracturing due to impact, friction and others. The complex phenomenon makes mathematical modelling and analysis a little difficult for this type of situation. Within this context, there is a need to formulate simple but accurate mathematical procedures in determining sufficient separation gaps of building structures to avoid structural pounding.

In this study, the geometric scaling factor (λ) of 1:30 is adopted for experimental shaking table and numerical tests on the scaled building models as mentioned earlier. Moreover, the scaling relationship between the natural frequency of the model (f_m) and natural frequency of the prototype (f_p) [54] is described as below.

$$\frac{f_m}{f_p} = \lambda^{-0.5} = 5.48 \tag{21}$$

The mathematical models to be used in a full scale are described as follows:

For low PGA level:

$$\hat{Y}_i = 30 \times (-50.7 - 0.0028 \times \frac{HT}{30} + 0.0066 \times \frac{HS}{30} + 600 \times E - 3.59 \times FT \times 5.48 - 0.46 \times FS \times 5.48 - 0.64 \times DT - 0.5 \times DS - 1210 \times E^2)$$

$$S = -1521 - 0.0028 \times HT + 0.0066 \times HS + 18000 \times E - 590.2 \times FT - 75.6 \times FS - 19.2 \times DT - 15 \times DS - 36300 \times E^2 \tag{22}$$

For moderate PGA level:

$$\hat{Y}_2 = 30 \times (16 - 0.002 \times \frac{HT}{30} + 0.008 \times \frac{HS}{30} + 3 \times E - 2.2 \times FT \times 5.48 - 0.24 \times FS \times 5.48 - 0.65 \times DT - 0.91 \times DS)$$

$$S = 480 - 0.002 \times HT + 0.008 \times HS + 90 \times E - 361.7 \times FT - 39.5 \times FS - 19.5 \times DT - 27.3 \times DS \quad (23)$$

For high PGA level:

$$\hat{Y}_2 = 30 \times (-0.83 - 0.009 \times \frac{HT}{30} + 0.024 \times \frac{HS}{30} + 49 \times E - 3.4 \times FT \times 5.48 - 0.6 \times FS \times 5.48 - DT - 1.2 \times DS)$$

$$S = -24.9 - 0.009 \times HT + 0.024 \times HS + 720 \times E - 559 \times FT - 98.6 \times FS - 30 \times DT - 36 \times DS \quad (24)$$

In high PGA level, the value of S that was derived from Equation 24 will be replaced with the value of $\hat{Y}_2$ in Equation 20. This is essential in the high PGA level only.

8.2. Worked Example

In order to estimate the separation gap between two adjacent buildings using Equations 22 to 24 in the real environment, structural engineers should first determine the structural characteristics including the height of the tall and short structure (HT, HS), the fundamental natural frequency of the tall and short structure (FT, FS), and the structural damping ratio of the tall and short structure (DT, DS). To determine the level of seismicity of the area, for low PGA level use Equation 22 is suggested, for moderate PGA level, Equation 23 is recommended and for high PGA level use Equations 24 and then 20 are the ones being proposed.

Let us assume a 13-storey building will be built next to an existing 7-storey building in Sydney, Australia. The height of the tall and short building is $HT = 39\ m$ and $HS = 21\ m$.

To estimate the building vibration period for the 13-storey and 7-storey buildings, the following equation given in the Australian Standard [49] code is used:

$$T = 1.25 k_t h^{0.75}$$

where T is the fundamental natural translational period of the structure, k_t depends on the structural type, it is 0.11 for moment-resisting steel frames and 0.075 for moment-resisting concrete frames; h is the height from the base of the structure to the uppermost seismic weight or mass, in metres.

Thus, the natural frequency of the 13-storey and 7-storey buildings are 0.466 and 0.7414 Hz respectively.

$$T_{13} = 1.25 \times 0.11 \times 39^{0.75} = 2.1458\ sec \Rightarrow f_{13} = 0.466\ Hz$$
$$T_7 = 1.25 \times 0.11 \times 21^{0.75} = 1.3488\ sec \Rightarrow f_7 = 0.7414\ Hz$$

For the purpose of this example, damping ratio of 5% is used for the two multi-storey buildings. Furthermore, Sydney Basin region is considered low risk seismic area. Present evaluation of earthquake risks in the Sydney area points out that on average, there is a 10 percent probability of ground acceleration surpassing 0.11g in 100 [73, 74]. However, in the above equations, values lower than 0.2g are ignored due to the very low level of PGA, which will have no impact or a very low impact on the structures.

Equation 22 is used to calculate the separation gap for low PGA level only. This is the only level that should be considered in the Sydney example. In calculating the separation gap between the two buildings in this example, the value of the PGA used was 0.2g. The separation gap of 154.32 mm was derived based on the said equation. On the other hand, the separation gap according to the Australian standard was found as in Equation (6). The calculated value of the separation gap based on the height of the tall building is 390 mm and 210 mm for the height of the short building. The calculations are anchored on the Australian standards as shown in Equation (6).

As can be gleaned from the example, the Australian Standard is adequately safe enough based on the low level of PGA. In other countries, high PGA levels need to consider multi variables to come up with a more accurate computation of the separation gap.

It is important to note that the proposed mathematical models presented in this study are specifically applicable to mid-rise steel frame buildings with unequal heights, assuming elastic structural response. Additionally, it is worth mentioning that soil-structure interaction was not considered in this study. The analysis proceeded under the assumption that the soil beneath the foundations is infinitely rigid. These assumptions and limitations should be considered when applying the findings of the study to real-world scenarios or when considering the broader context of soil-structure interaction.

9. Conclusions

This study aimed to determine the required minimum separation gaps between mid-rise steel-frame buildings to avoid potential collisions during seismic excitation. The investigation into the determination of the minimum safe distance to avoid earthquake-induced pounding has been conducted for the coupled scaled models of 15 & 10-story buildings, 15 & 5-storey buildings, and 10 & 5-storey buildings. The outcomes of this investigation were dedicated to using multiple regression analysis to develop mathematical equations to estimate the minimum separation gap between two adjacent buildings to preclude earthquake-induced pounding. Experimental tests and numerical analyses were conducted to derive mathematical equations using data analytics and prediction techniques. In order to verify the accuracy of the models, the results of the numerical analysis have been compared with the results of experimental measurements.

The earthquake characteristics, the parameters of the buildings, and the numerical separation gaps have been defined as inputs in the regression analysis. The results of the study revealed that the separation gap is directly proportional to the height of the short building (HS) and the earthquake peak ground acceleration (E). Moreover, the computed separation gap is inversely proportional to the height of the tall building (HT), the frequency of the tall building (FT), the frequency of the short building (FS), the damping ration of the tall building (DT), and the damping ration of the short building (DS).

The findings clearly indicate that the proposed mathematical model developed in this study can be effectively used to determine the required minimal gap between two adjacent buildings to prevent or avoid their collisions during different seismic excitations. Furthermore, it was revealed that some parameters have a higher impact on the separation gaps when compared with other parameters. The parameter HS has a higher impact than HT, and DS has a higher impact than DT. These proved that short building characteristics play a major role in ascertaining the minimum separation gap to avoid pounding between adjacent structures during earthquakes. The equation formulated for low and moderate PGA levels was a multiple linear equation, while the equation for the high PGA level was a polynomial equation.

The practical application of the proposed mathematical model for simulation purposes in predicting adequate separation gaps between adjacent buildings to avoid earthquake-induced pounding requires knowledge of the model's parameters.

In this study, the values of the parameters have been determined based on the results of experiments conducted to determine the minimum separation gaps between adjacent edifices to prevent structural pounding. However, it is also highly recommended that more extensive experimental studies be done to evaluate the range of the model's parameters more accurately for various types of structures with different material and contact surface geometry properties. Several parameters have been neglected in this study, e.g., the P-delta effect, soil structure interaction, direction of incidence of earthquakes, structural systems, etc. Further studies, taking these parameters into consideration, are recommended. As a result, this study is suggested to be used as a reference for the engineering industry in using the concluded mathematical equations so they can estimate the minimum required separation gap between adjacent buildings.

10. Declarations

10.1. Author Contributions

Conceptualization, Y.J.; methodology, Y.J. and H.F.; software, Y.J.; validation, Y.J. and H.F.; formal analysis, Y.J.; investigation, Y.J.; resources, Y.J. and H.F.; data curation, Y.J.; writing—original draft preparation, Y.J.; writing—review and editing, H.F. and M.M.; visualization, Y.J.; supervision, H.F. and M.M.; project administration, Y.J.; funding acquisition, Y.J. and H.F. All authors have read and agreed to the published version of the manuscript.

10.2. Data Availability Statement

The data presented in this study are available in the article.

10.3. Funding

The authors received no financial support for the research, authorship, and/or publication of this article.

10.4. Conflicts of Interest

The authors declare no conflict of interest.

11. References

[1] Miari, M., Choong, K. K., & Jankowski, R. (2019). Seismic pounding between adjacent buildings: Identification of parameters, soil interaction issues and mitigation measures. Soil Dynamics and Earthquake Engineering, 121, 135–150. doi:10.1016/j.soildyn.2019.02.024.

[2] Jankowski, R. (2015). Pounding between Superstructure Segments in Multi-Supported Elevated Bridge with Three-Span Continuous Deck under 3D Non-Uniform Earthquake Excitation. Journal of Earthquake and Tsunami, 9(4), 1550012. doi:10.1142/S1793431115500128.

[3] Khatami, S. M., Naderpour, H., Barros, R. C., Jakubczyk-Gałczyńska, A., & Jankowski, R. (2019). Effective formula for impact damping ratio for simulation of earthquake-induced structural pounding. Geosciences (Switzerland), 9(8), 347. doi:10.3390/geosciences9080347.

[4] Abdel Raheem, S. E., Hayashikawa, T., & Dorka, U. (2011). Ground motion spatial variability effects on seismic response control of cable-stayed bridges. Earthquake Engineering and Engineering Vibration, 10(1), 37–49. doi:10.1007/s11803-011-0045-5.

[5] Abdel Raheem, S. E. (2009). Pounding mitigation and unseating prevention at expansion joints of isolated multi-span bridges. Engineering Structures, 31(10), 2345–2356. doi:10.1016/j.engstruct.2009.05.010.

[6] Luo, Y., Li, Y., Wang, X., & Lu, G. (2021). Influence of Restrainer Piers on the Seismic Performance of Long Bridges with Equal-Height Piers. Mathematical Problems in Engineering, 2021. doi:10.1155/2021/6651215.

[7] Rosenblueth, E., & Meli, R. (1986). The 1985 Mexico earthquake. Concrete international, 8(5), 23-34.

[8] Kasai, K., & Maison, B. F. (1997). Building pounding damage during the 1989 Loma Prieta earthquake. Engineering Structures, 19(3), 195–207. doi:10.1016/S0141-0296(96)00082-X.

[9] Anagnostopoulos, S. A. (1996, June). Building pounding re-examined: how serious a problem is it. Eleventh world conference on earthquake engineering, 23-28 June, 1996, Acapulco, Mexico.

[10] Lin, J., & Weng, C. (2002). A study on seismic pounding probability of buildings in Taipei metropolitan area. Journal of the Chinese Institute of Engineers, 25(2), 123–135. doi:10.1080/02533839.2002.9670687.

[11] Lin, C. C. J., Hung, H. H., Liu, K. Y., & Chai, J. F. (2010). Reconnaissance observation on bridge damage caused by the 2008 Wenchuan (China) earthquake. Earthquake Spectra, 26(4), 1057–1083. doi:10.1193/1.3479947.

[12] Kazemi, F., Miari, M., & Jankowski, R. (2021). Investigating the effects of structural pounding on the seismic performance of adjacent RC and steel MRFs. Bulletin of Earthquake Engineering, 19(1), 317–343. doi:10.1007/s10518-020-00985-y.

[13] Cole, G., Dhakal, R., Carr, A. J., & Bull, D. (2010). Building pounding state of the art: Identifying structures vulnerable to pounding damage. 2010 New Zealand Society of Earthquake Engineerings (NZSEE) Conference, 26-28 March, 2010, Wellington, New Zealand.

[14] Sekkour, H., Belounar, L., Belounar, A., Boussem, F., & Fortas, L. (2022). A Triangular Shell Element Based on Higher-order Strains for the Analysis of Static and Free Vibration. Civil Engineering Journal, 8(10), 2096-2109. doi:10.28991/CEJ-2022-08-10-06.

[15] Efraimiadou, S., Hatzigeorgiou, G. D., & Beskos, D. E. (2013). Structural pounding between adjacent buildings subjected to strong ground motions. Part I: The effect of different structures arrangement. Earthquake Engineering & Structural Dynamics, 42(10), 1509-1528. doi:10.1002/eqe.2285.

[16] Raheem, S. E. A., Fooly, M. Y. M., Omar, M., & Zaher, A. K. A. (2019). Seismic pounding effects on the adjacent symmetric buildings with eccentric alignment. Earthquake and Structures, 16(6), 715–726. doi:10.12989/eas.2019.16.6.715.

[17] Polycarpou, P. C., Papaloizou, L., & Komodromos, P. (2014). An efficient methodology for simulating earthquake-induced 3D pounding of buildings. Earthquake Engineering and Structural Dynamics, 43(7), 985–1003. doi:10.1002/eqe.2383.

[18] Leibovich, E., Rutenberg, A., & Yankelevsky, D. Z. (1996). On eccentric seismic pounding of symmetric buildings. Earthquake Engineering and Structural Dynamics, 25(3), 219–233. doi:10.1002/(SICI)1096-9845(199603)25:3<219::AID-EQE537>3.0.CO;2-H.

[19] Jankowski, R. (2008). Earthquake-induced pounding between equal height buildings with substantially different dynamic properties. Engineering Structures, 30(10), 2818–2829. doi:10.1016/j.engstruct.2008.03.006.

[20] Jankowski, R. (2010). Experimental study on earthquake-induced pounding between structural elements made of different building materials. Earthquake Engineering & Structural Dynamics, 39(3), 343–354. doi:10.1002/eqe.941.

[21] Kazemi, F., Mohebi, B., & Yakhchalian, M. (2020). Predicting the seismic collapse capacity of adjacent structures prone to pounding. Canadian Journal of Civil Engineering, 47(6), 663–677. doi:10.1139/cjce-2018-0725.

[22] Raheem, S. A., Fooly, M. Y., Shafy, A. A., Abbas, Y. A., Omar, M., Latif, M. M. S. A., & Mahmoud, S. (2018). Seismic pounding effects on adjacent buildings in series with different alignment configurations. Steel and Composite Structures, 28(3), 289-308. doi:10.12989/scs.2018.28.3.289.

[23] Anagnostopoulos, S. A. (1988). Pounding of buildings in series during earthquakes. Earthquake Engineering & Structural Dynamics, 16(3), 443–456. doi:10.1002/eqe.4290160311.

[24] Skrekas, P., Sextos, A., & Giaralis, A. (2014). Influence of bi-directional seismic pounding on the inelastic demand distribution of three adjacent multi-storey R/C buildings. Earthquake and Structures, 6(1), 71–87. doi:10.12989/eas.2014.6.1.071.

[25] Sołtysik, B., & Jankowski, R. (2013). Non-linear strain rate analysis of earthquake-induced pounding between steel buildings. International Journal of Earth Sciences and Engineering, 6(3), 429–433.

[26] Elwardany, H., Seleemah, A., & Jankowski, R. (2017). Seismic pounding behavior of multi-story buildings in series considering the effect of infill panels. Engineering Structures, 144, 139–150. doi:10.1016/j.engstruct.2017.01.078.

[27] Khatami, S. M., Naderpour, H., Barros, R. C., Jakubczyk-Gałczyńska, A., & Jankowski, R. (2020). Determination of peak impact force for buildings exposed to structural pounding during earthquakes. Geosciences (Switzerland), 10(1), 18. doi:10.3390/geosciences10010018.

[28] Anagnostopoulos, S. A. (1995). Earthquake induced pounding: State of the art. Proceedings of the 10th European Conference on Earthquake Engineering, 28 August-2 September, 1995, Vienna, Austria.

[29] ICBO. (1997). Uniform building code. International Conference of Building Officials, California, United States.

[30] EN 1998-1:2004. (2004). Design of structures for earthquake resistance-part 1: General rules, seismic actions and rules for buildings. European Committee for Standardization, Brussels, Belgium.

[31] IBC. (2009). International Building Code. International Code Council, Illinois, United States.

[32] Jeng, V., Kasai, K., & Maison, B. F. (1992). A Spectral Difference Method to Estimate Building Separations to Avoid Pounding. Earthquake Spectra, 8(2), 201–223. doi:10.1193/1.1585679.

[33] Penzien, J. (1997). Evaluation of building separation distance required to prevent pounding during strong earthquakes. Earthquake Engineering & Structural Dynamics, 26(8), 849–858. doi:10.1002/(SICI)1096-9845(199708)26:8<849::AID-EQE680>3.0.CO;2-M.

[34] Lopez-Garcia, D., & Soong, T. T. (2009). Assessment of the separation necessary to prevent seismic pounding between linear structural systems. Probabilistic Engineering Mechanics, 24(2), 210–223. doi:10.1016/j.probengmech.2008.06.002.

[35] Filiatrault, A., & Cervantes, M. (1995). Separation between buildings to avoid pounding during earthquakes. Canadian Journal of Civil Engineering, 22(1), 164–179. doi:10.1139/l95-015.

[36] Garcia, D. L. (2004). Separation between adjacent nonlinear structures for prevention of seismic pounding. Proceedings of the 13th World Conference on Earthquake Engineering, 1-6 August, 2004, Vancouver, Canada.

[37] Hong, H. P., Wang, S. S., & Hong, P. (2003). Critical building separation distance in reducing pounding risk under earthquake excitation. Structural Safety, 25(3), 287–303. doi:10.1016/s0167-4730(02)00080-2.

[38] Wang, S. S., & Hong, H. P. (2006). Quantiles of critical separation distance for nonstationary seismic excitations. Engineering Structures, 28(7), 985–991. doi:10.1016/j.engstruct.2005.11.003.

[39] Khatami, S. M., Naderpour, H., Barros, R. C., & Jankowski, R. (2019). Verification of Formulas for Periods of Adjacent Buildings Used to Assess Minimum Separation Gap Preventing Structural Pounding during Earthquakes. Advances in Civil Engineering, 2019. doi:10.1155/2019/9714939.

[40] Naderpour, H., Khatami, S. M., & Barros, R. C. (2017). Prediction of critical distance between two MDOF systems subjected to seismic excitation in terms of artificial neural networks. Periodica Polytechnica Civil Engineering, 61(3), 516–529. doi:10.3311/PPci.9618.

[41] Shrestha, B. (2013). Effects of separation distance and nonlinearity on pounding response of adjacent structures. International Journal of Civil and Structural Engineering, 3(3), 603.

[42] Favvata, M. J. (2017). Minimum required separation gap for adjacent RC frames with potential inter-story seismic pounding. Engineering Structures, 152, 643–659. doi:10.1016/j.engstruct.2017.09.025.

[43] Barbato, M., & Tubaldi, E. (2013). A probabilistic performance-based approach for mitigating the seismic pounding risk between adjacent buildings. Earthquake Engineering and Structural Dynamics, 42(8), 1203–1219. doi:10.1002/eqe.2267.

[44] Abdel Raheem, S. E. (2014). Mitigation measures for earthquake induced pounding effects on seismic performance of adjacent buildings. Bulletin of Earthquake Engineering, 12(4), 1705–1724. doi:10.1007/s10518-014-9592-2.

[45] Khatami, S. M., Naderpour, H., Mortezaei, A., Razavi, S. M. N., Lasowicz, N., & Jankowski, R. (2021). Effective gap size index for determination of optimum separation distance preventing pounding between buildings during earthquakes. Applied Sciences (Switzerland), 11(5), 1–15. doi:10.3390/app11052322.

[46] Tena-Colunga, A., & Sánchez-Ballinas, D. (2022). Required building separations and observed seismic pounding on the soft soils of Mexico City. Soil Dynamics and Earthquake Engineering, 161, 107413, 1-33. doi:10.1016/j.soildyn.2022.107413.

[47] Kamal, M., & Inel, M. (2022). Simplified approaches for estimation of required seismic separation distance between adjacent reinforced concrete buildings. Engineering Structures, 252, 113610. doi:10.1016/j.engstruct.2021.113610.

[48] Kamal, M., & Inel, M. (2022). A new equation for prediction of seismic gap between adjacent buildings located on different soil types. Journal of Building Engineering, 57, 104784. doi:10.1016/j.jobe.2022.104784.

[49] AS1170.4. (2007). Structural Design Actions Part 4: Earthquake Actions in Australia. Standards Australia, Sydney, Australia.

[50] Jaradat, Y., Sobhi, P., & Far, H. (2023). An investigation into adequacy of separation gap to preclude earthquake-induced pounding. Structural Engineering and Mechanics, 86(1), 29–48. doi:10.12989/sem.2023.86.1.029.

[51] Jaradat, Y., Far, H., & Saleh, A. (2021). Examining the adequacy of separation gaps between adjacent buildings under near-field and far-field earthquakes. The Thirteenth International Conference on Earthquake Resistant Engineering Structures, 26–28 May, 2021.

[52] AS/NZS3678. (2011). Structural steel—Hot-rolled plates, floorplates and slabs. Standards Australia, Sydney, Australia.

[53] Tabatabaiefar, S., Fatahi, B., & Samali, B. (2014). Numerical and experimental investigations on seismic response of building frames under influence of soil-structure interaction. Advances in Structural Engineering, 17(1), 109–130. doi:10.1260/1369-4332.17.1.109.

[54] Tabatabaiefar, H. R., & Mansoury, B. (2015). Detail design, building and commissioning of tall building structural models for experimental shaking table tests. The Structural Design of Tall and Special Buildings, 25(8), 357–374. doi:10.1002/tal.1262.

[55] Tabatabaiefar, H. R. (2016). Detail design and construction procedure of laminar soil containers for experimental shaking table tests. International Journal of Geotechnical Engineering, 10(4), 328–336. doi:10.1080/19386362.2016.1145419.

[56] Chopra A. (2007). Dynamics of Structures (3rd Ed.). Prentice Hall, New Jersey, United States.

[57] Saleh, A., Far, H., & Mok, L. (2018). Effects of different support conditions on experimental bending strength of thin walled cold formed steel storage upright frames. Journal of Constructional Steel Research, 150, 1–6. doi:10.1016/j.jcsr.2018.07.031.

[58] Jaradat, Y., & Far, H. (2023). Impact Stiffness of Linear Viscoelastic Model for Seismic Pounding Simulation: An Experimental Evaluation. Civil Engineering Journal (Iran), 9(6), 1289–1311. doi:10.28991/CEJ-2023-09-06-01.

[59] Kramer S. L. (1996). Geotechnical earthquake engineering. Prentice Hall, New Jersey, United States.

[60] K-karamodin, A., & H-Kazemi, H. (2010). Semi-active control of structures using neuro-predictive algorithm for MR dampers. Structural Control and Health Monitoring, 17(3), 237–253. doi:10.1002/stc.278.

[61] Computers and Structures INC (CSI). (2000). SAP2000 Integrated Software for Structural Analysis and Design. Computers and Structures Inc., Berkeley, United States.

[62] Jaradat, Y., Far, H., & Mortazavi, M. (2022). Experimental Evaluation of Theoretical Impact Models for Seismic Pounding. Journal of Earthquake Engineering, 2022, 1–21. doi:10.1080/13632469.2022.2131654.

[63] Jaradat Y, & Far H. (2021). Project Title: Seismic Behaviour of High-rise and Mid-rise Buildings. University of Technology Sydney, Australia

[64] Far, H., & Flint, D. (2017). Significance of using isolated footing technique for residential construction on expansive soils. Frontiers of Structural and Civil Engineering, 11(1), 123–129. doi:10.1007/s11709-016-0372-8.

[65] Jaradat, Y., & Far, H. (2021). Optimum stiffness values for impact element models to determine pounding forces between adjacent buildings. Structural Engineering and Mechanics, 77(2), 293–304. doi:10.12989/sem.2021.77.2.293.

[66] Kutner, M. H., Nachtsheim, C. J., Neter, J., & Li, W. (2005). Applied linear statistical models. McGraw-Hill, New York, United States.

[67] Far, C., & Far, H. (2019). Improving energy efficiency of existing residential buildings using effective thermal retrofit of building envelope. Indoor and Built Environment, 28(6), 744–760. doi:10.1177/1420326X18794010.

[68] Shao, J. (1993). Linear model selection by cross-validation. Journal of the American Statistical Association, 88(422), 486–494. doi:10.1080/01621459.1993.10476299.

[69] Cox, D. R. (1984). Interaction. International Statistical Review, 52(1), 1-24. doi:10.2307/1403235.

[70] Ostertagová, E. (2012). Modelling using polynomial regression. Procedia Engineering, 48, 500–506. doi:10.1016/j.proeng.2012.09.545.

[71] Jeng, V., Kasai, K., & Jagiasi, A. (1992). The separation to avoid seismic pounding. Proceedings of the Tenth World Conference on Earthquake Engineering, 19-24 July, Madrid, Spain.

[72] Kasai, K., Jagiasi, A. R., & Jeng, V. (1996). Inelastic Vibration Phase Theory for Seismic Pounding Mitigation. Journal of Structural Engineering, 122(10), 1136–1146. doi:10.1061/(asce)0733-9445(1996)122:10(1136).

[73] Denham, D. (1992). Earthquake attack in the Sydney basin: What is the risk? Exploration Geophysics, 23(4), 579–587. doi:10.1071/EG992579.

[74] Zhang, X., & Far, H. (2022). Effects of dynamic soil-structure interaction on seismic behaviour of high-rise buildings. Bulletin of Earthquake Engineering, 20(7), 3443–3467. doi:10.1007/s10518-021-01176-z.

Appendix I

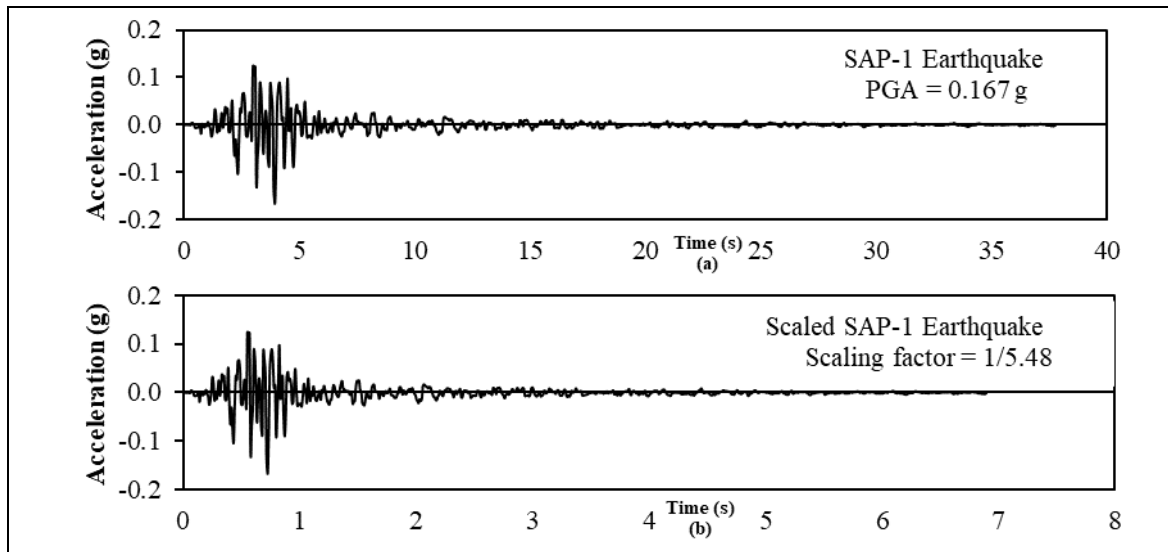Selected earthquake acceleration-time histories.

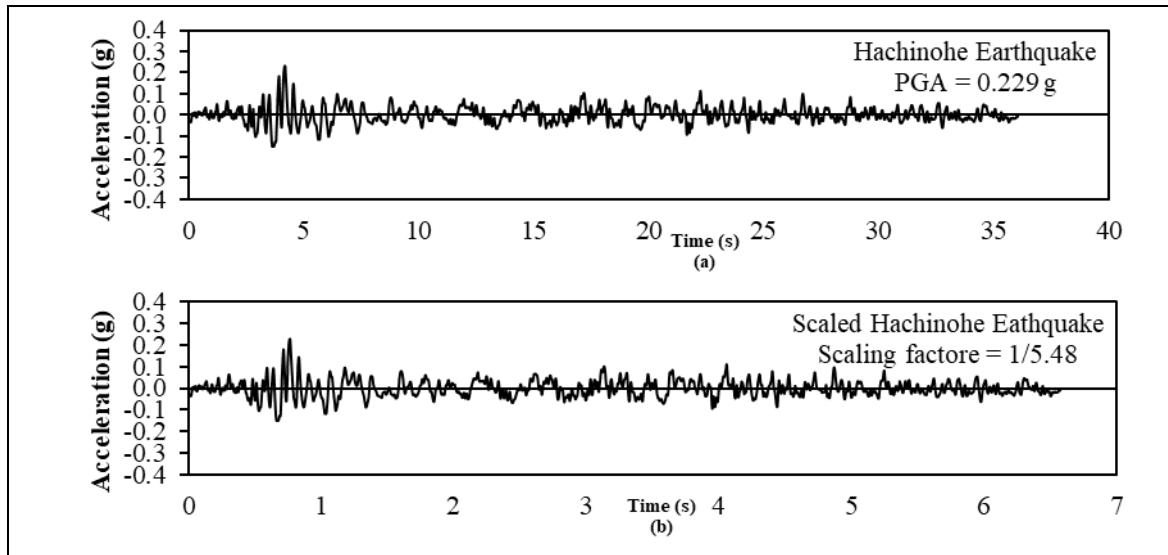**Figure A-1. SAP-1 earthquake; a) Original record, b) Scaled record**

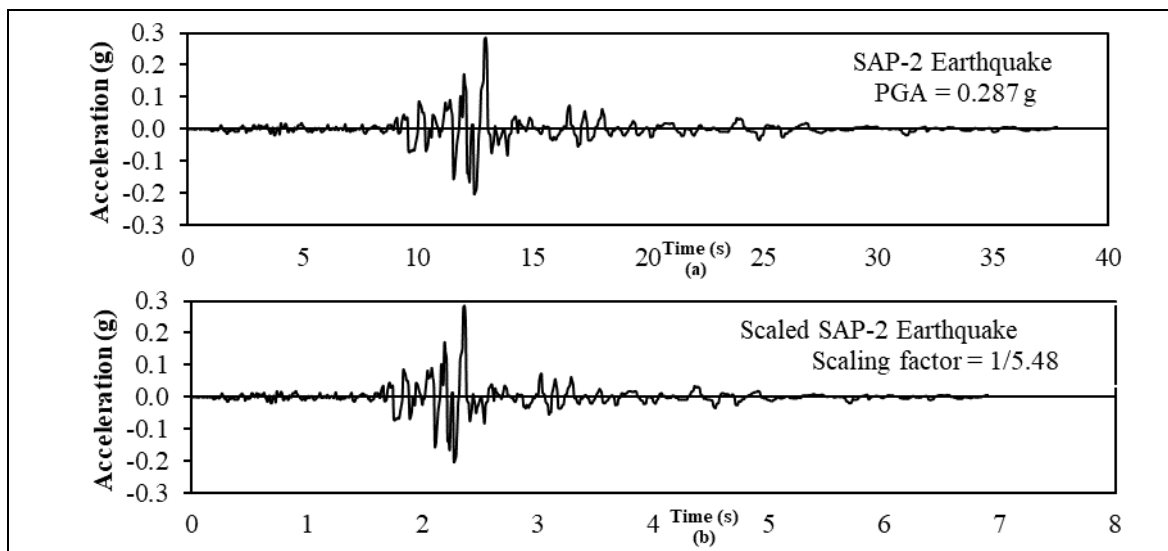**Figure A-2. Hachinohe earthquake 1968; a) Original record, b) Scaled record**

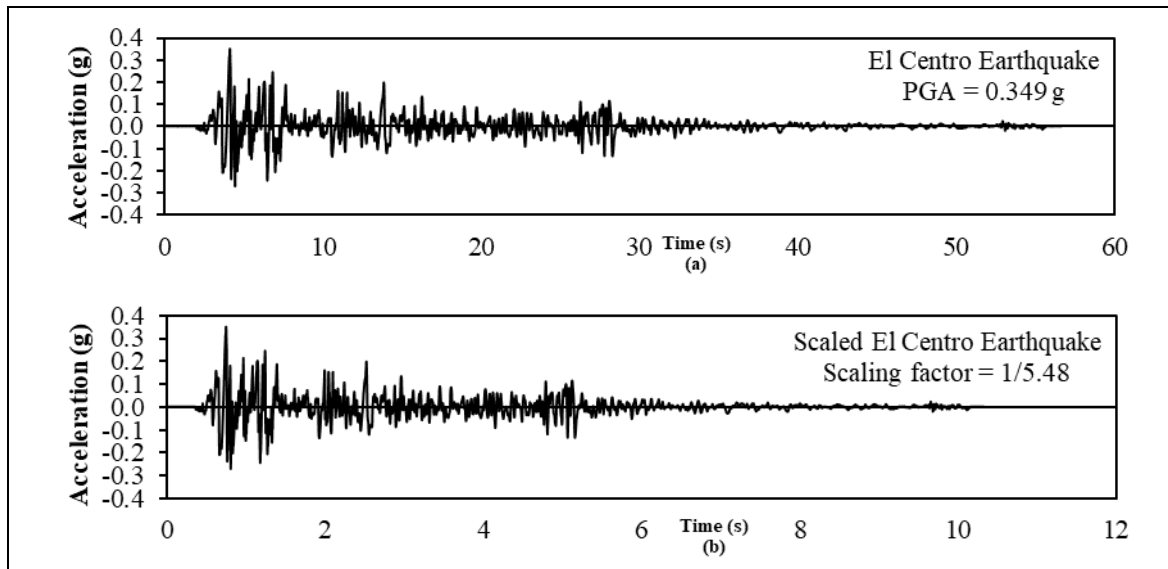**Figure A-3. SAP-2 earthquake; a) Original record, b) Scaled record**

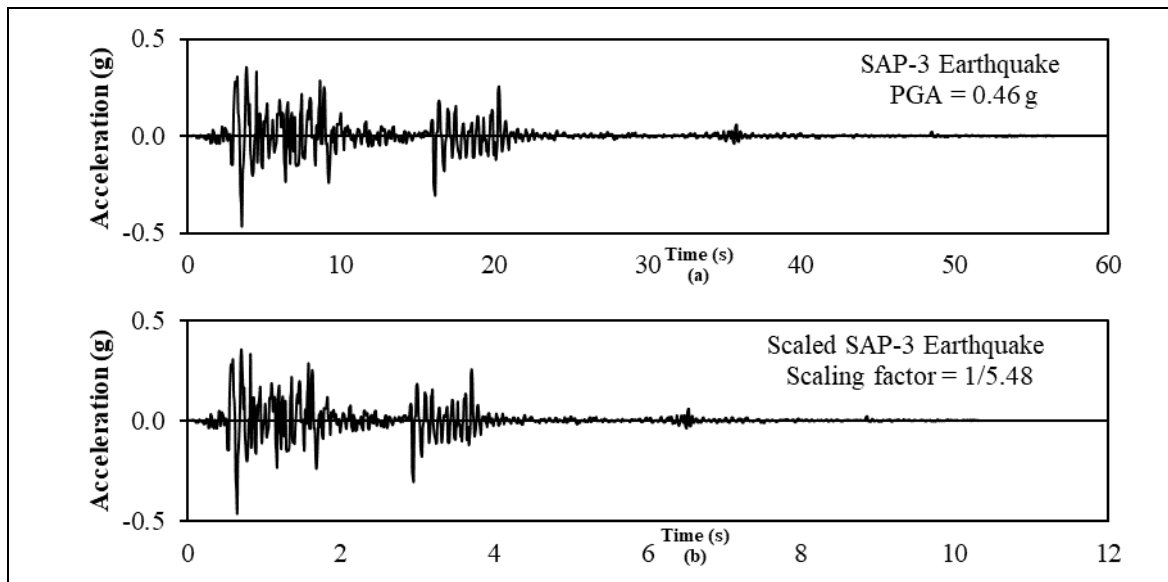**Figure A-4. El Centro earthquake 1940; a) Original record, b) Scaled record**

Figure A-5. SAP-3 earthquake; a) Original record, b) Scaled record
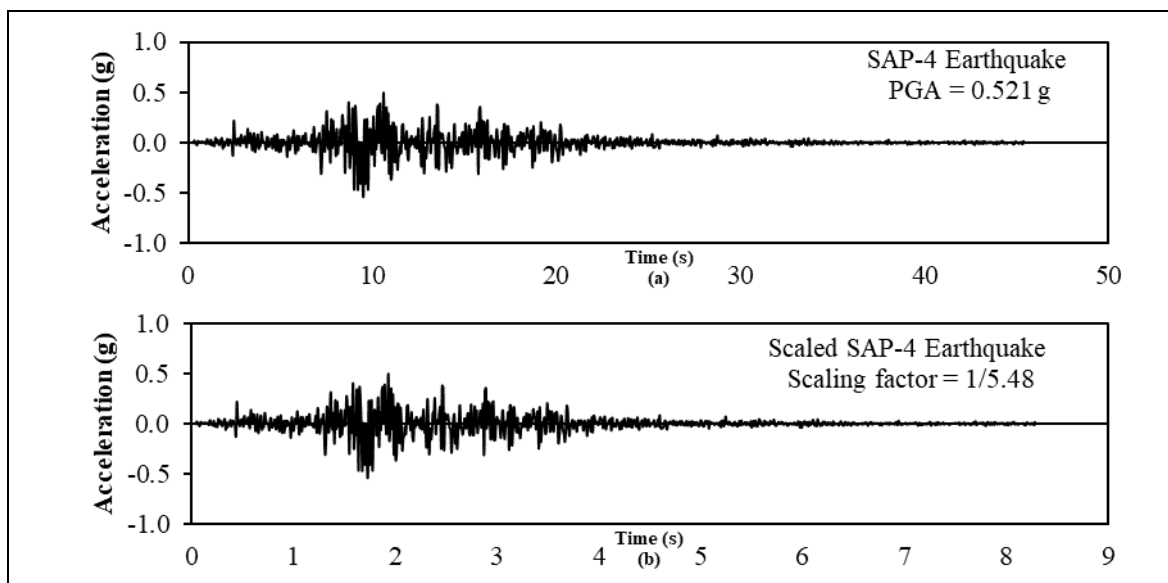

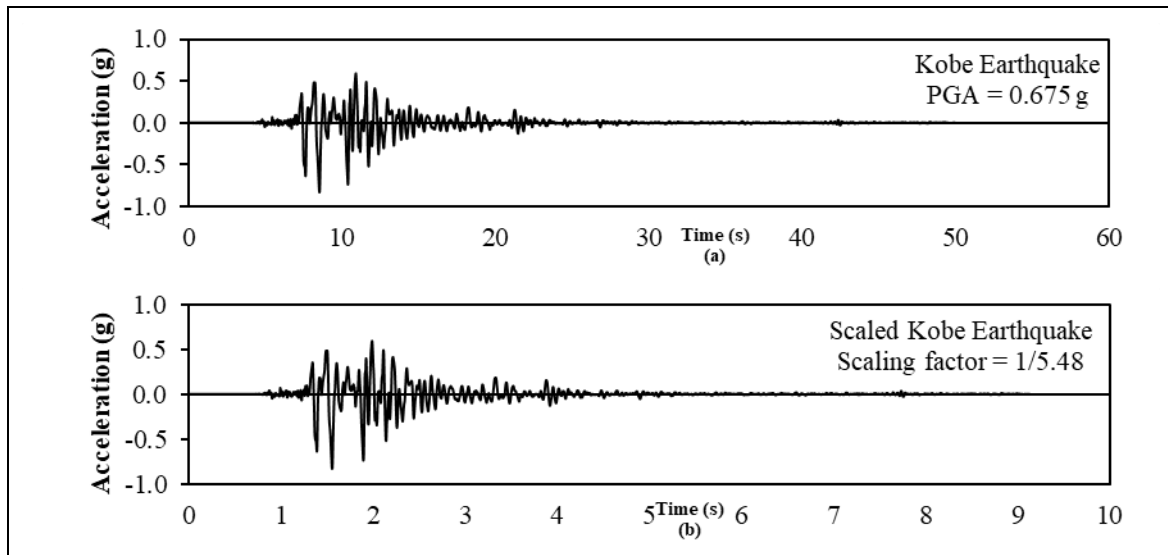**Figure A-6. SAP-4 earthquake; a) Original record, b) Scaled record**

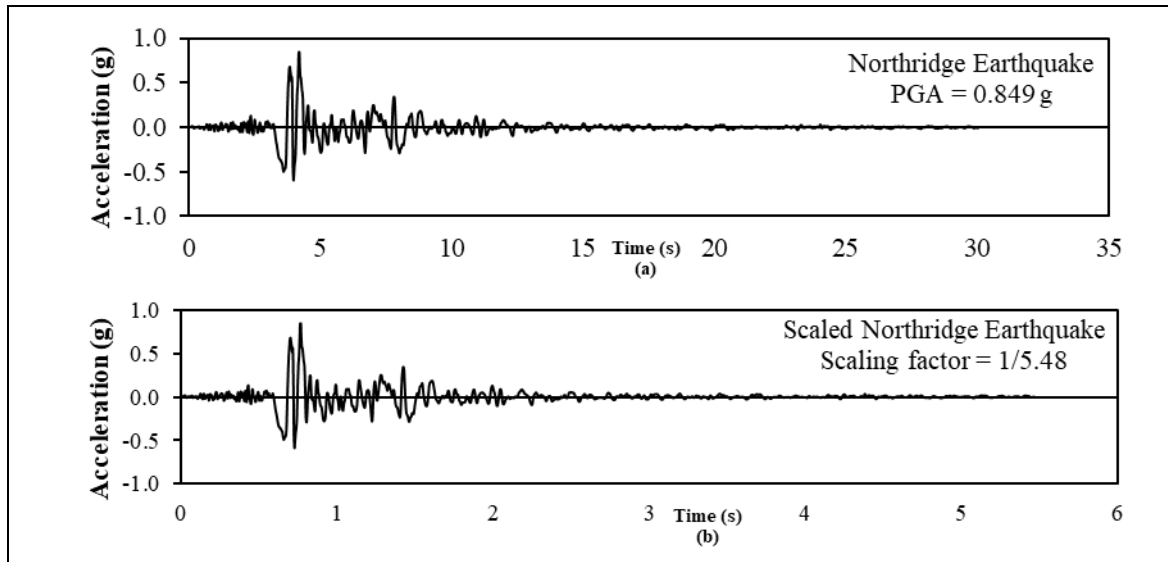**Figure A-7. Kobe earthquake 1995; a) Original record, b) Scaled record**

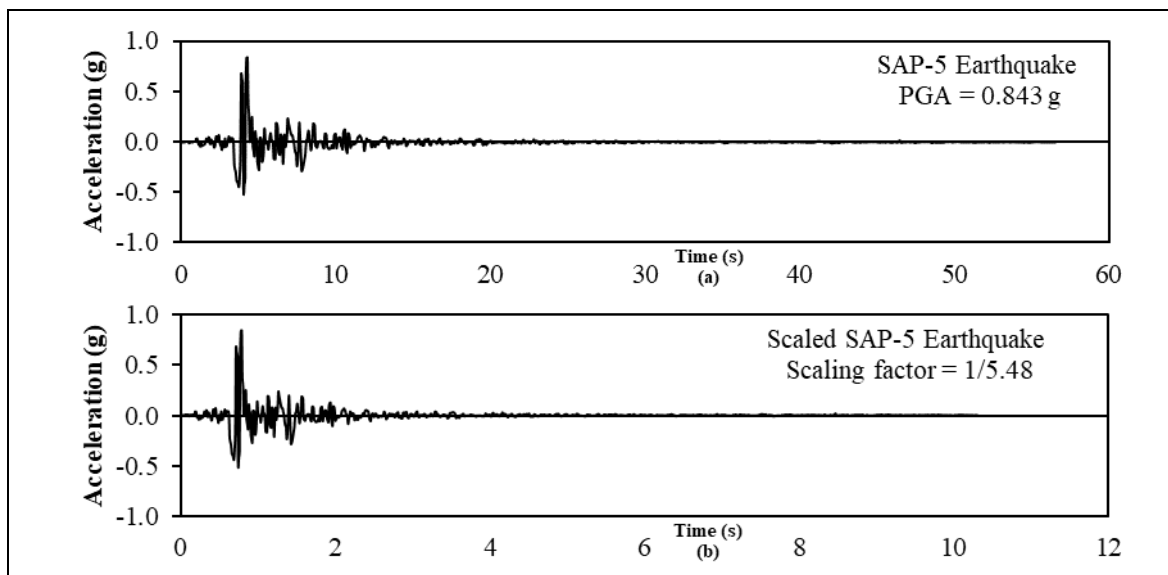**Figure A-8 Northridge earthquake 1994; a) Original record, b) Scaled record**

Figure A-9. SAP-5 earthquake; a) Original record, b) Scaled record

Appendix II

		Numerical min gap mm	Height Tall mm	Height Short mm	PGA g	Frequency Tall Hz	Frequency Short Hz	Damping Tall %	Damping Short %	Stiffness Tall kN/mm	Stiffness Short kN/mm	Mass Tall kg	Mass Short kg
Numerical min gap mm	Pearson Corre	1	0.253	0.481	0.434	-0.338	-0.526	-0.121	-0.062	-0.304	-0.480	0.296	0.574
	Sig. (2-tailed)	-	0.000	0.000	0.000	0.000	0.000	0.000	0.001	0.000	0.000	0.000	0.000
	N	3081	3081	3081	3081	3081	3081	3081	3081	3081	3081	3081	3081
Height Tall mm	Pearson Corre	0.253	1	0.425	-0.028	-0.821	-0.372	0.136	-0.066	**-0.957**	-0.420	0.526	0.359
	Sig. (2-tailed)	0.000	-	0.000	0.121	0.000	0.000	0.000	0.000	0.000	0.000	0.000	0.000
	N	3081	3081	3081	3081	3081	3081	3081	3081	3081	3081	3081	3081
Height Short mm	Pearson Corre	0.481	0.425	1	-0.009	-0.349	**-0.932**	0.058	-0.047	-0.406	**-1.00**	0.224	**0.884**
	Sig. (2-tailed)	0.000	0.000	-	0.623	0.000	0.000	0.001	0.009	0.000	0.000	0.000	0.000
	N	3081	3081	3081	3081	3081	3081	3081	3081	3081	3081	3081	3081
PGA g	Pearson Corre	0.434	-0.028	-0.009	1	0.015	-0.013	0.007	0.046	0.027	0.017	-0.006	0.020
	Sig. (2-tailed)	0.000	0.121	0.623	-	0.406	0.482	0.708	0.010	0.131	0.359	0.727	0.263
	N	3081	3081	3081	3081	3081	3081	3081	3081	3081	3081	3081	3081
Frequency Tall Hz	Pearson Corre	-0.338	-0.821	-0.349	0.015	1	0.313	-0.099	0.039	**0.899**	0.345	**-0.890**	-0.301
	Sig. (2-tailed)	0.000	0.000	0.000	0.406	-	0.000	0.000	0.029	0.000	0.000	0.000	0.000
	N	3081	3081	3081	3081	3081	3081	3081	3081	3081	3081	3081	3081
Frequency Short Hz	Pearson Corre	-0.526	-0.372	-0.932	-0.013	0.313	1	-0.061	0.072	0.356	**0.933**	-0.204	**-0.956**
	Sig. (2-tailed)	0.000	0.000	0.000	0.482	0.000	-	0.001	0.000	0.000	0.000	0.000	0.000
	N	3081	3081	3081	3081	3081	3081	3081	3081	3081	3081	3081	3081
Damping Tall %	Pearson Corre	-0.121	0.136	0.058	0.007	-0.099	-0.061	1	0.010	-0.127	-0.058	0.071	0.058
	Sig. (2-tailed)	0.000	0.000	0.001	0.708	0.000	0.001	-	0.568	0.000	0.001	0.000	0.001
	N	3081	3081	3081	3081	3081	3081	3081	3081	3081	3081	3081	3081
Damping Short %	Pearson Corre	-0.062	-0.066	-0.047	0.046	0.039	0.072	0.010	1	0.064	0.045	-0.019	-0.098
	Sig. (2-tailed)	0.001	0.000	0.009	0.010	0.029	0.000	0.568	-	0.000	0.012	0.287	0.000
	N	3081	3081	3081	3081	3081	3081	3081	3081	3081	3081	3081	3081
Stiffness Tall kN/mm	Pearson Corre	-0.304	-0.957	-0.406	0.027	0.899	0.356	-0.127	0.064	1	0.401	-0.640	-0.343
	Sig. (2-tailed)	0.000	0.000	0.000	0.131	0.000	0.000	0.000	0.000	-	0.000	0.000	0.000
	N	3081	3081	3081	3081	3081	3081	3081	3081	3081	3081	3081	3081
Stiffness Short kN/mm	Pearson Corre	-0.480	-0.420	-1.00	0.017	0.345	0.933	-0.058	0.045	0.401	1	-0.221	**-0.885**
	Sig. (2-tailed)	0.000	0.000	0.000	0.359	0.000	0.000	0.001	0.012	0.000	-	0.000	0.000
	N	3081	3081	3081	3081	3081	3081	3081	3081	3081	3081	3081	3081
Mass Tall kg	Pearson Corre	0.296	0.526	0.224	-0.006	-0.890	-0.204	0.071	-0.019	-0.640	-0.221	1	0.196
	Sig. (2-tailed)	0.000	0.000	0.000	0.727	0.000	0.000	0.000	0.287	0.000	0.000	-	0.000
	N	3081	3081	3081	3081	3081	3081	3081	3081	3081	3081	3081	3081
Mass Short kg	Pearson Corre	0.574	0.359	0.884	0.020	-0.301	-0.956	0.058	-0.098	-0.343	-0.885	0.196	1
	Sig. (2-tailed)	0.000	0.000	.000	0.263	0.000	0.000	0.001	0.000	0.000	0.000	0.000	-
	N	3081	3081	3081	3081	3081	3081	3081	3081	3081	3081	3081	3081